Preparation and Characterization of TiO_2-Based Nano Particles and Tests for Their Activities in Methylene Blue Photodegradation

Aoshu Duan

Thesis submitted to the
Faculty of Graduate and Postdoctoral Studies
in partial fulfillment of the requirements for the degree of

Master of Applied Science

Under the auspices of the Chemical & Biological Engineering

Abstract

A two-step hydrothermal method was applied to synthesis Vanadium Sulfide (IV) coupled with commercial P25 on TiO_2 nanoparticle (VS_4-on-P25). Materials were characterized by scanning electron microscope (SEM), high-resolution transmission electron microscopy (HRTEM), X-ray diffraction (XRD), ultraviolet–visible spectroscopy (UV-Vis), diffuse reflectance UV-Vis spectroscopy and Raman spectroscopy. Photocatalytic activity of this new material was determined by photo-degradation of Methylene blue (MB) under UV irradiation. Experiments show that the VS_4-on-P25 exhibits a higher photocatalytic activity than commercial P25 by providing more active site for dye adsorption, and reducing the recombination of charge carriers. Furthermore, the VS_4-on-P25 extends its light-absorption spectrum into visible-light range due to its narrower band gap. The highest photocatalytic activity was found with a VS_4 loading of 6 wt.%, which outperforms pure P25 by a factor of 2.29 in MB degradation rate.

Résumé

Un procédé hydrothermal en deux étapes a été utilisé pour la synthèse du sulfure de vanadium (IV) couplé avec la nanoparticule commerciale P25 TiO_2 (VS_4-sur-P25). Les matériaux ont été caractérisées par la microscopie électronique à balayage (MEB), la microscopie électronique à transmission haute résolution (HRTEM), la diffraction des rayons X (XRD), la spectroscopie ultraviolet-visible (UV-Vis), la spectroscopie par réflectance diffuse UV-Vis et la spectroscopie Raman. Le rendement photocatalytique a été déterminé par la photo-dégradation du bleu de méthylène sous irradiation UV. Les expériences montrent que la VS_4-on-P25 présente une activité photocatalytique supérieure à celle du P25 commercial en fournissant plus de sites actifs pour l'adsorption de colorant, et en réduisant la recombinaison des porteurs de charge. En outre, le VS_4-on-P25 étend son spectre d'absorption de lumière dans la plage de lumière visible en rétrécissant sa largeur de bande. Le rendement photocatalytique le plus élevé a été trouvé à une charge de VS_4 de 6 poids.%, ce qui surpasse le P25 pur d'un facteur de 2,29 du bleu de méthylène sous irradiation UV.

Acknowledgment

I would like to express the deepest appreciation to the people who helped me during the study period both in University of Ottawa and University of Waterloo.

First of all, I would like to acknowledge my supervisor, Dr Jason Zhang, for providing me with the opportunity to work on this project of photocatalyst. His support and guidance were of great help to me during the past two years.

I am grateful to my co-supervisor, Dr. Aiping Yu of University of Waterloo for making this project possible by providing the laboratory, generously sharing equipment, and for providing information on the field of semiconductors and photocatalysts. I would also like to acknowledge Dr. Zhongwei Chen for his guidance during my 11-mouth stay in University of Waterloo.

I would like to acknowledge lab members from Dr. Yu's group for the help they provided in my experiments and in writing my thesis. I am particularly grateful to Gregory Lui and Dr. Jinyun Liao for their precious support and disinterested help on this project. I would like to acknowledge Mica Peng for her assistance on bilingual editing.

Last but not least, I want to thank all the colleagues and my family for their supports and encouragements.

Nomenclature

CB	conduction band
EPR	electron paramagnetic resonance
EV	electron volt
FESEM	field-emission scanning electron microscopy
GC/MS	gas chromatography/mass spectrometry
HRTEM	high-resolution transmission electron microscopy
JCPDS	joint committee on powder diffraction standards
LC/MS	liquid chromatography/mass spectrometry
MB	Methylene blue
SC	semiconductor
SEM	scanning electron microscope
TAA	Thioacetamide
TMD	transition-metal dichalcogenide
UV	ultraviolet
UV-Vis	ultraviolet–visible spectroscopy
VB	valence band
XRD	X-ray diffraction

Contents

Table of Figures

List of Tables

1. Introduction

Since Fujishima [1] first reported the photoelectrochemical water-splitting on Titanium Dioxide (TiO_2) electrode in 1972, this environmental friendly chemical approach has quickly become a hot research topic in numerous areas such as anti-bacteria coating [2, 3], self-cleaning materials [4, 5], hydrogen generation [1, 6-8], and especially air [3, 9-11] or water[12-14] purification due to its implications for solar energy conversion.

The very first documented study on photocatalytic phenomenon can be traced back to 1921 [15], when Renz reported discolorations of TiO_2 and some other metal oxides during illumination with sunlight. But not until Fujishima's milestone discovery in 1972 [1], the mechanism of photocatalysed reactions was postulated. Generally speaking, a photocatalysed reaction takes place at the surface of the capable semiconductor photocatalyst/photocatalysts under certain illumination. Photogenerated electrons transfer from the valence band to the conduction band (e_{cb}^{-}) by the driving of absorbed photon energy, result in positively charged holes left in the valence band (h_{vb}^{+}). Electrons and holes travel to the surface of the photocatalysis simultaneously and evenly, participate in reduction and oxidation reactions with the reactants respectively. The basic expression of this procedure can be written as Reaction (1.1):

$$TiO_2 + h\nu = e_{cb}^{-} + h_{vb}^{+} \quad \ldots\ldots\ldots\ldots\ldots\ldots\ldots\ldots\ldots \quad (1\text{-}1)$$

A large number of different photocatalysts have been investigated over the last several decades. Most of them are transition-metal oxides or sulphides semiconductors such as TiO_2 [1], ZnO [16], WO_3 [17], $SrTiO_3$ [18], α -Fe_2O_3 [19], ZnS [20], CdS [21], CdSe [22] and PbS [23]. Among all the candidate semiconductors, TiO_2 is one of the first discovered and also most intensively studied photocatalysts worldwide. Highly photo-active, remarkably stable, non-toxic, and more importantly, inexpensive, all these characteristics [24] render TiO_2 as the most promising photocatalyst to satisfy the need of future industrial scale use.

TiO_2 photocatalysts however can only be solely activated under ultraviolet (UV) irradiation, which accounts for only about 5% of the total solar spectrum. Moreover, the efficiency of photon-to-electron conversion is greatly limited by electron and hole recombination: during which, large amounts of energy loss in the form of heat [25]. These considerations currently limit the practical applications of TiO_2 photocatalysts, and comprise the most pertinent technical challenges that must be addressed.

It is therefore highly desirable to extend the absorbance spectrum of TiO_2 photocatalysts to visible light range. With the recent progress in nano semiconductor science and technology, several different methods have been investigated to raise the visible light response of TiO_2 by introducing impurities and defects to the photocatalyst/photocatalysts system. These methods include metal [26, 27] and/or[28] non-metal [29, 30] ion doping, surface deposition of noble metal [31, 32], emiconductor coupling [33, 34], and photosensitization of photocatalysts [35, 36].

Nano-scaled few layered transition-metal dichalcogenides (TMD), or transition-metal disulfides TC_2, in which T is a transition-metal element from groups 4 IVB to 10 VIIIB and C is a chalcogen (be specific, the sulphur predominantly) [37]. As shown in Figure1-1, sixteen transition-metal elements and three chalcogen elements are highlighted in the periodic table as yellow and magenta, respectively, indicates that those elements are proven for crystallizing the layered transition-metal dichalcogenides. Several known forms of TC_2 [38-54] are frequently reported in the field of photoelectron chemistry due to their excellent electrical and catalytic activities. These materials are widely considered as potential coupling semiconductor alternatives for enhancing conventional photocatalysts' visible-light photoactivity [24, 43, 55]. One thing should be noticed is that layered structure TMDs may not exist in every combination between a "yellow" element and a "magenta" element: e.g. $NiTe_2$ is typically layer-structured [56] while NiS_2 is found to be a pyrite unit cell structure due to the existing of S_2^{2-} dimer [45].

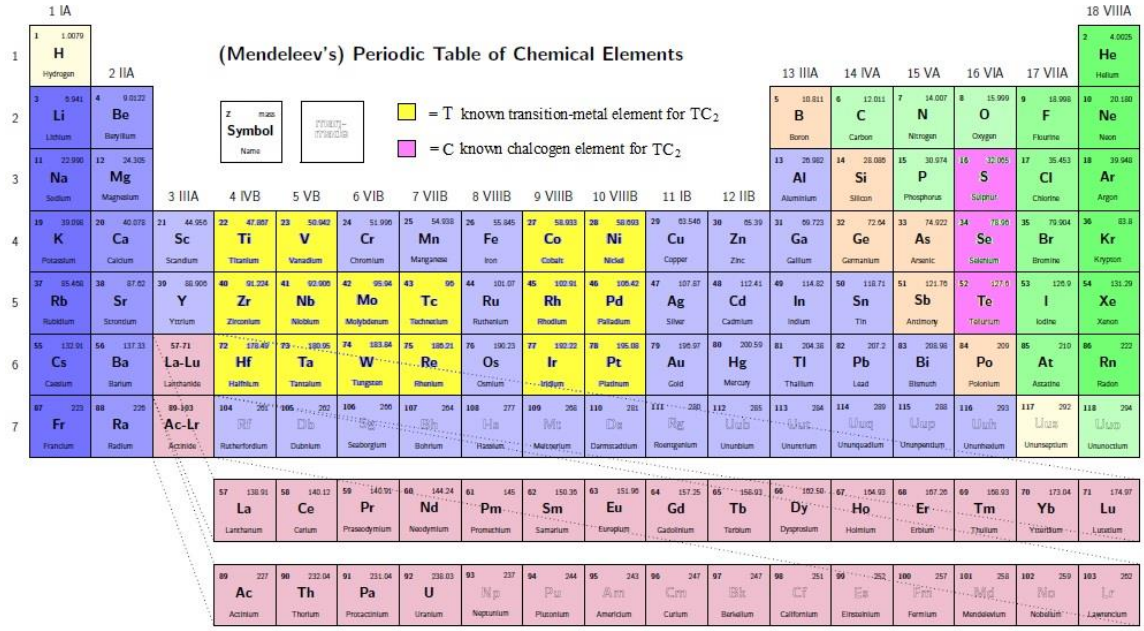

Figure 1-1 Known TMDs in Periodic table of chemical elements

Among these TMDs, Vanadium Disulfide (VS_2) has been studied in many different areas such as batteries [57], supercapacitors [58], and sensors [59] due to its high conductivity and low band gap. However, the difficulties and complexities of VS_2 synthesis, particularly nano-scaled VS_2, greatly limit its research progress. On the other hand, Patrónite (VS_4) is another Vanadium Sulfide with the formula $V^{4+}(S_2^{2-})_2$. The "linear-chain" structured VS_4 shares some similarities with VS_2 crystal, making it a possible succedaneum of VS_2.

In this study, we report a two-step solvo/hydrothermal process for first synthesis VS_4 nanodiscs, and then introducing the VS_4 to the surface of type P25 TiO_2 nano particles (a

commercially available TiO_2 nano particle, the average diameter of P25 nano particles is 21 nm) to form VS4-on-P25 heterostructures. Scanning electron microscope (SEM) characterized the morphology of VS_4 material, high-resolution transmission electron microscopy (HRTEM), X-ray diffraction (XRD) further confirmed the crystal structure and chemical composition of VS_4 and VS_4-on-P25, ultraviolet–visible spectroscopy (UV-Vis) is used to detect the Methylene blue (MB) concentration during the photodegradation study, while diffuse reflectance UV-Vis spectroscopy is applied to measure the light-absorbing spectrum of synthesized materials. Raman spectroscopy of VS_4 nanomaterials is also reported in this thesis. Photocatalytic activity was determined by the photo-degradation of MB under UV irradiation. Results showed that the VS_4-on-P25 exhibits a higher photocatalytic activity than commercial P25 in MB photodegradation. This is attributed to the coupled highly conductive, nanodiscs structural VS_4, which provides a planar conjugated surface for dye adsorption, contributes charge transfer with its high conductivity, and increases photon to charge-carrier conversion by narrower the band gap of VS_4-on-P25 material.

This thesis is divided into six chapters: Chapter 1, the introduction, which provides an overview of the project outline and background; Chapter 2, the literature review on TiO_2 photocatalytic reactions, which includes the properties of TiO_2 materials, and the mechanisms and dynamics of photocatalysts, especially the TiO_2 assisted MB dye photodegradation reactions; Chapter 3, the literature review of photocatalysis enhancement methods, mainly focusing on doping and coupling. Also layered TMDs and VS_4 would be briefly introduced in this section; Chapter 4, the experimental section of this study;

Chapter 5 characterizations and the photocatalytic activity test of VS_4-on-P25. Conclusions and future works for this study would be summarized in Chapter 6, as the last Chapter of this thesis.

2. TiO_2 Photocatalytic Reactions

2.1 Crystal Structures of TiO_2

There are 3 major polymorphs of TiO_2 in nature: rutile, anatase and less-commonly seen brookite [60]. Among them, rutile and anatase are crystals while brookite is orthorhombic [61]. Since most previous work on TiO_2 has been focused on rutile and anatase, the emphasis of this chapter is on those two.

It is an undeniable fact that different phases of TiO_2 differ in activities for photocatalytic reactions. A universally recognized conclusion is that the photocatalytic activity of anatase is superior to that of rutile. The advantages of anatase include high density of localized states and small grain size, restricting the energy loss caused by electron-hole recombination [62-64]. This allows for more effective provision of charge carriers by the anatase, resulting in higher photocatalytic efficiency compared to rutile. Even more advantageous aspects of anatase are that, in general terms, anatase has a higher surface energy than rutile due to its smaller grain size [65, 66], leading to a more attractive surface for the reactants to attach.

However, it is too costly to synthesize or separate phase-pure TiO_2 in anatase [67-69]. Besides, as previously mentioned in Chapter 1, rather than the difference in photocatalytic activity between different crystal phases, the main factor that restricts TiO_2 photocatalysts'

applications is its narrow light-absorption spectrum which all phases of TiO_2 material suffer from.

Due to (110) (Figure 2-1 a) and (100) (Figure 2-1 b) crystal faces which are low in energy, rutile is more thermodynamically stable than any other polymorphs of TiO_2 [70]. The (110) terraces is the most stable face. Each Oxygen atom bridges two Titanium atoms, while each Titanium atom coordinates six Oxygen atoms. Five-coordinated Titanium atoms can be found parallel located to the lines of bridging Oxygen atoms.

Similar to (110) surface, the parallel Oxygen atoms and five-coordinate Titanium atoms structure exists in (100) surface as well. However, the more distorted spatial arrangement of those atoms increases the total energy of (110) surface, resulting in less thermodynamic stability.

The high energy (001) (Figure 2-1 c) crystal face–is the most unstable face. Rows of double-coordinated Oxygen atoms and five-coordinated Titanium atoms are being arranged alternatively in (001) surface. High temperature would disturb this weak orientation: Ramamoorthy and Vanderbilt [71] reported that starting at 475 ℃, the (001) surface would experience a phase re-structure transition.

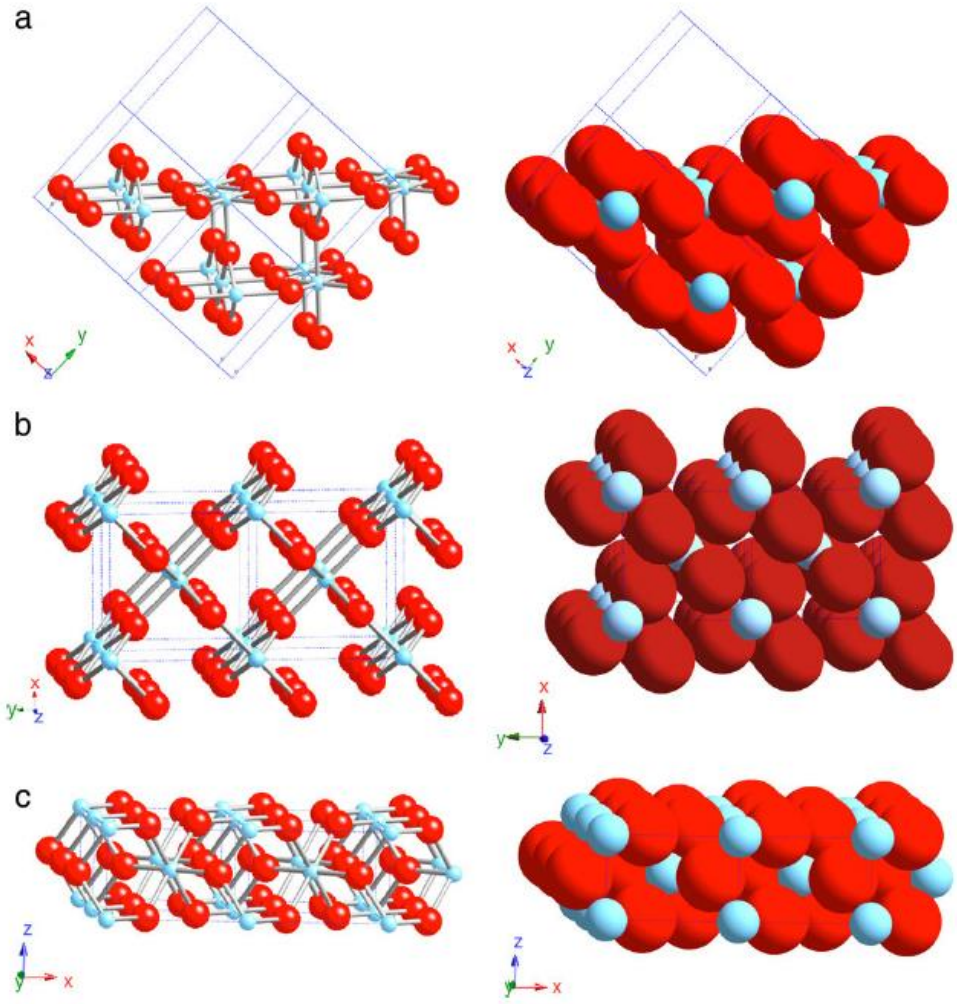

Figure 2-1 Schematic representations of selected low-index faces of rutile: (a) (110); (b) (100); and (c) (001) [61]

Anatase is another one of the two major mineral forms of titanium dioxide, in which low energy (101) (Figure 2-2 a) and (001) (Figure 2-2 b) surfaces exist naturally [72]. In (101) crystal faces, undulating geometrically arranged five-coordinated Titanium atoms and bridging Oxygen atoms with intervals are located in every two parallel rows. Also, the (101) crystal face is the most commonly seen and thermodynamically stable surface in

anatase [63], the surface energy of anatase (101) crystal face is proven to be even lower in surface energy than the rutile (110) face [70]. The atom configuration in (001) crystal face is more flat but less stable compared to (101) surface.

The unusually seen (100) surface (Figure 2-2 c), consists of two parallel rows of double-coordinated Oxygen atoms and one row of five-coordinated Titanium atoms, respectively. Both (001) and (100) crystal faces are unstable thermodynamically, phase re-structure transitions can be observed among those two surfaces [72-74].

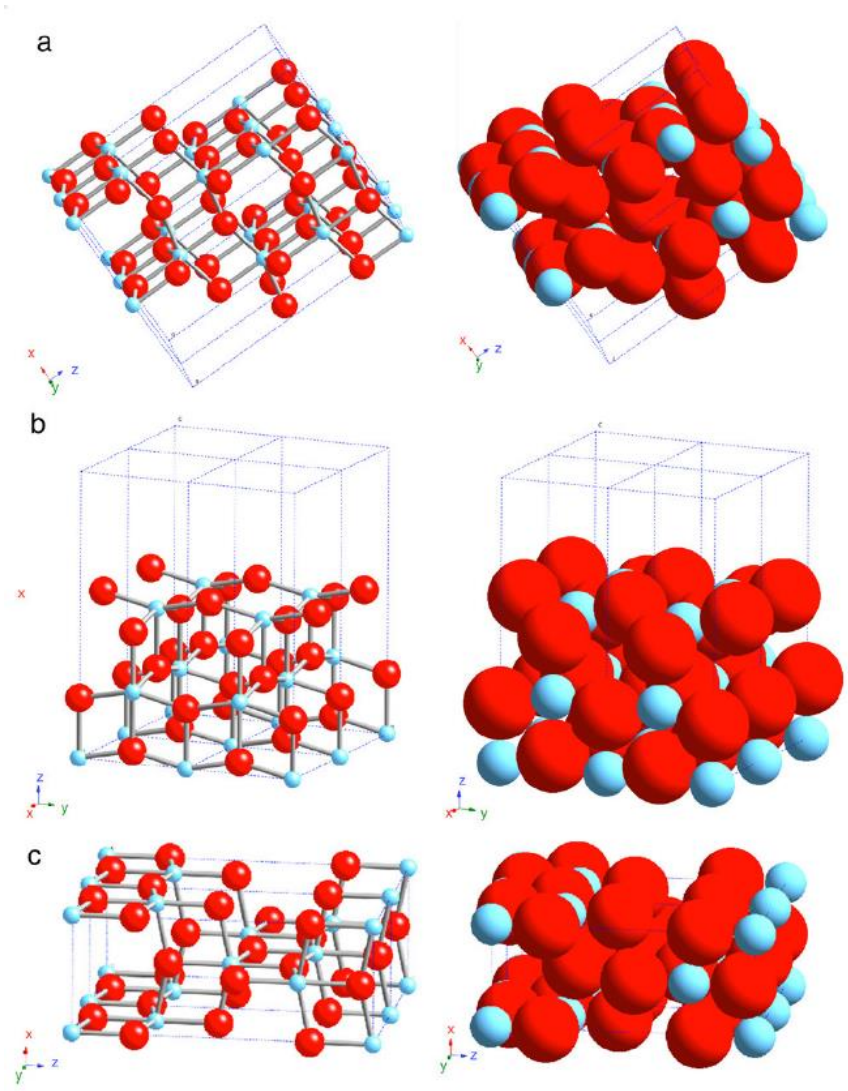

Figure 2-2 Schematic representations of selected low-index faces of anatase: (a) (110); (b) (001); and (c) (100) [61]

2.2 Mechanism of Photocatalysis

As discussed in the introduction, it took almost half a century for generations of researchers to reveal the reaction mechanism of photocatalysis [1, 15, 75-77]. Essentially, photocatalysis is an energy conversion process [78]: first, light energy which carried by

photons is transferred into chemical energy carried by free radicals. And then, a specific chemical reaction would be accelerated since free radicals can lower the activation energy of the reaction. In a heterogeneous TiO_2 photocatalysis system, this process can be fundamentally described as:

$$TiO_2 + h\nu = e_{cb}^- + h_{vb}^+ \quad (2\text{-}1)$$

$$O_2 + 4H^+ + 4e_{cb}^- = 2H_2O \quad (2\text{-}2)$$

$$2H_2O + 4h_{vb}^+ = O_2 + 4H^+ \quad (2\text{-}3)$$

Where e_{cb}^- and h_{vb}^+ are respective electrons in the conduction band and the electrons vacancy in the valence band.

To achieve a photocatalysis process, the photon energy has to be equal or higher than the band gap of the photocatalyst. Under this irradiation, a hole in valence band can be formed. Meanwhile, to balance the total charge, a photo-activated electron escapes from the conduction band to fill the valence band. Thus electron-hole pairs can be generated. Then, the electrons and holes travel to the photocatalyst surface separately, where electrons are trapped by oxidants/acceptors while holes are trapped by reductants/donors. The interface between photocatalyst and reactants can provide the path for these charged free radicals to participate in secondary reactions, in which electrons can cause reduction while holes can take part in oxidation. One thing should be noticed here, not all the photo-generated electrons and holes contribute the photocatalysis process; charge recombination occurs

both in bulk and at the surface of the photocatalysts. Figure 2-3 depicts the process of photocatalysis.

Study on interface and colloid chemistry further expounding the mechanism of photocatalysis. As Table 2-1 shows the characteristic time for each stages of reaction in TiO_2 photocatalysis.

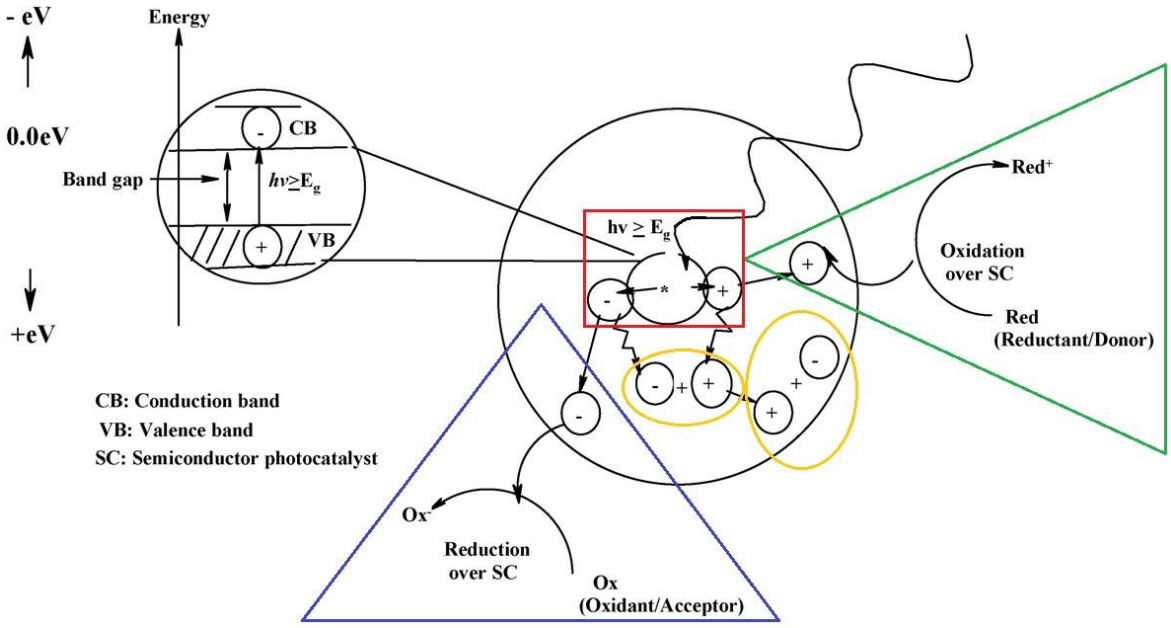

Figure 2-3 Schematic of photocatalysis process, (red) photo-generation of electron &hole pair (green) hole trapping and oxidation of donor/reductant at photocatalyst surface (blue) electron trapping and reduction of oxidant/acceptor at photocatalyst surface (yellow) electron and hole recombination in the bulk and at surface of photocatalyst [88]

Table 2-1 Characteristic time for primary stages of reaction in TiO_2 photocatalysis

Primary process	Chemical Equation	Time	Comments
Charge carrier generation	$TiO_2 + hv = e_{cb}^- + h_{vb}^+$	fs	Extremely fast indirect transition, It is impossible and meaningless to quantitative measure nowadays [24, 79]
Charge trapping	$e_{cb}^- \rightarrow e_{tr}^-$	~500 ps[80]	The deeper electrons/holes travel, the more time it takes for trapping
	$h_{vb}^+ \rightarrow h_{tr}^+$	~100 ps[80]	
Charge recombination	$h_{tr}^+ + e_{cb}^- \rightarrow HEAT$	1-25 μs[81, 82]	Besides heat, Photons might be generated in recombination as well
	$e_{tr}^- + h_{vb}^+ \rightarrow HEAT$		
Interfacial charge transfer	$h_{tr}^+ + Organic\ Molecule \rightarrow Oxidized\ Molecule^{\cdot+}$	ps, ns, μs	The transfer rate is varied for different organic molecules [83-86]
	$e_{tr}^- + O_2 = O_2^{\cdot-}$	ns, μs, ms	The transfer rate is varied for different organic molecules. However, this process is always slower than the transfer of holes [80-82, 87, 88]

2.3 Mechanism of TiO_2 Photodegradation MB Dye

One of the most important and promising applications for TiO_2 photocatalyst is to purify water by decomposing and mineralizing the organic compounds [89-92]. Studies have shown that a large number of the organic pollutants are TiO_2-photodegradable, including alkanes [93, 94], haloalkanes [95, 96], alkenes [97, 98], aromatics [99, 100], aliphatic hydrocarbons[101, 102], heterocyclic compounds [103, 104], herbicides [105-107], pesticides [103, 108, 109], and dyes [110-112].

Methylene blue (MB), molecular formula $C_{16}H_{18}N_3SCl$ (Figure 2-4 a), is a heterocyclic aromatic chemical compound. It is a dark green powdery solid at room temperature while its aqueous solution is blue. The maximum light absorption for MB can be observed around 664-666 nm, as Figure 2-4 (b) shows. MB is unstable and colorless when exposed to a reducing agent, and it is widely used as biological and chemical indicator in numerous areas, e.g. analytical chemistry [113-115] and biochemistry [116-118] redox indicator.

The photodegradation study of MB aqueous solution under UV [30, 119, 120] or visible light [121-123] irradiation is one of the most fundamental and convenient methods to investigate the activity of a TiO_2 photocatalyst.

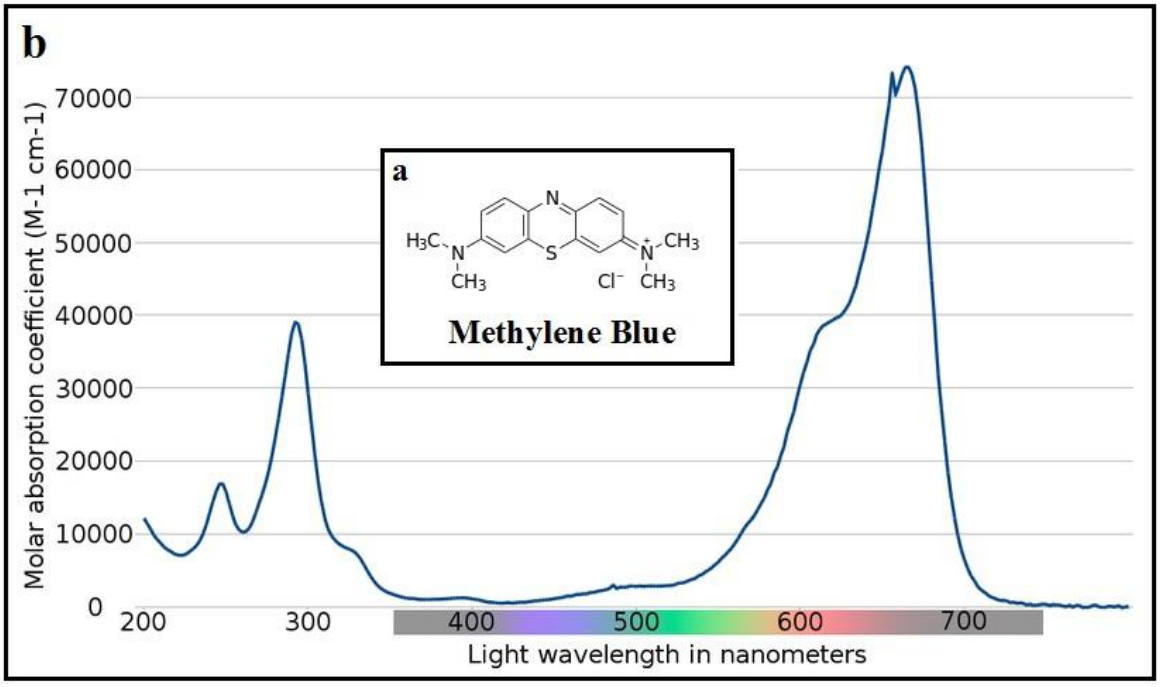

Figure 2-4 Chemical formula and light-absorbance spectrum of MB

The mechanism of photodegradation in heterogeneous TiO_2 photocatalysis system for different kinds of organic molecules can be acquired in many studies [124-126]. In general, the mechanism can be written as an extension of the basic equations described earlier in this review. A scheme re-edited from Ref. [127] shows the photodegradation pathway of MB:

1. Electron and hole generation

See Equation (2-1)

2. Oxygen free radical generation (by electron)

$$(O_2)_{ads} + e_{cb}^- = O_2^{\bullet -} \quad \text{..... (2-4)}$$

3. Hydroxy free radical generation (by hole)

$$(H_2O \Leftrightarrow H^+ + OH^-)_{ads} + h^+_{vb} = H^+ + OH^{\bullet} \quad \text{..... (2-5)}$$

4. Neutralization of hydroperoxyl free radical (by Oxygen free radical)

$$O_2^{\circ -} + H^+ = HO_2^{\circ} \quad \text{..... (2-6)}$$

5. Disproportionation of hydroperoxyl free radical

$$2HO_2^{\circ -} = H_2O_2 + O_2 \quad \text{..... (2-7)}$$

6. Decomposition of hydrogen peroxide (by electron)

$$H_2O_2 + e^- = OH^{\circ} + OH^- \quad \text{..... (2-8)}$$

7. Oxidation of the organic reactant (by hydroxyl free radical)

$$R + OH^{\circ} = R'^{\bullet} + H_2O \quad \text{..... (2-9)}$$

8. Formation of degradation product

$$R + h^+ = R^{+\circ} = P_D \quad \text{..... (2-10)}$$

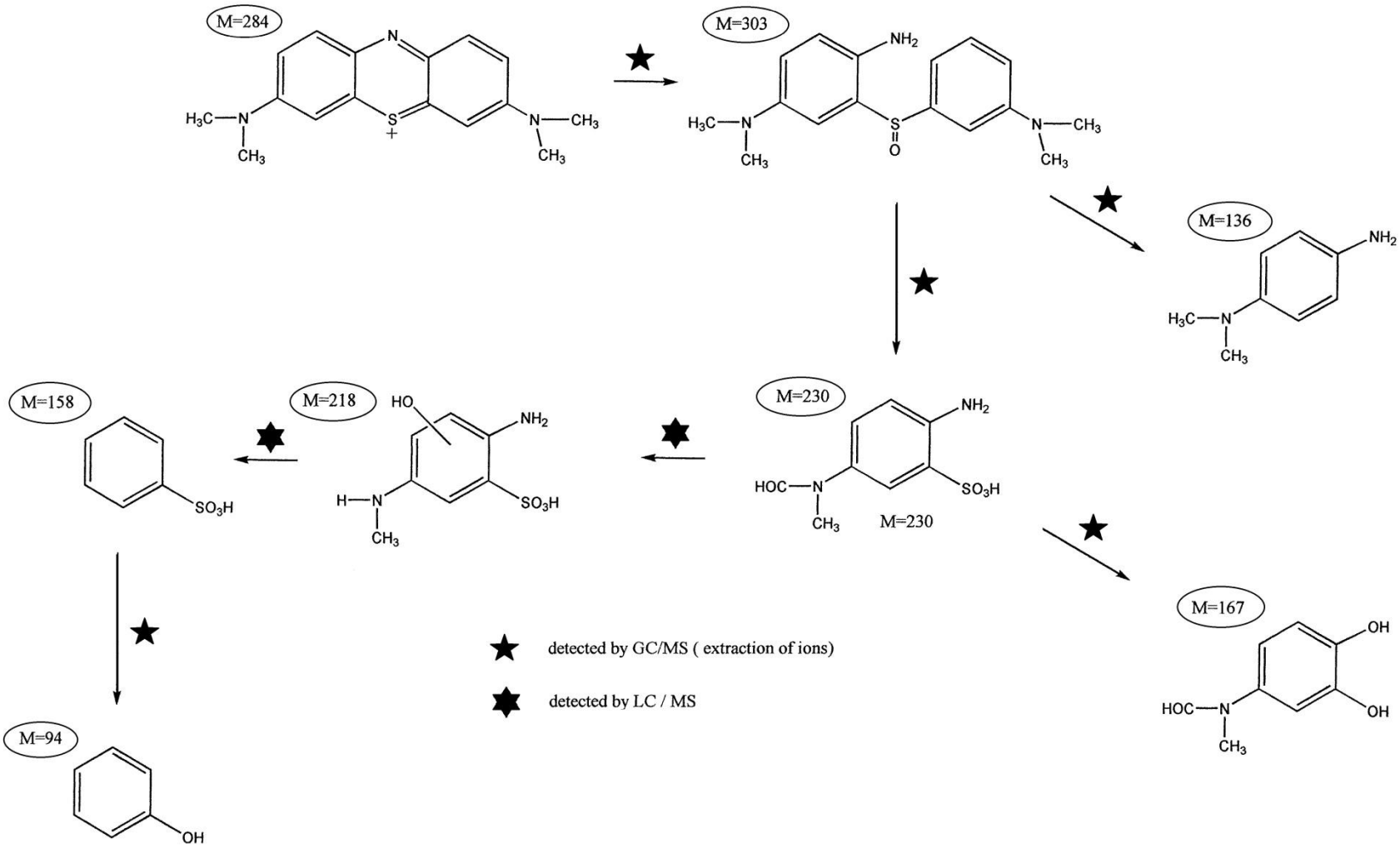

Figure 2-5 Scheme of MB degradation pathway [127]

2.4 Kinetics of TiO_2 Photodegradation MB Dye

To put it simply, the entire heterogeneous TiO_2 assisted MB photodegradation reaction proceeds following 3 steps as listed, 1. TiO_2 adsorbs the MB. 2. Reaction occurs at the interface between them. 3. The colorless product detaches from the TiO_2 surface.

Adsorption of MB on TiO_2

Adsorption is the necessary prerequisite to a photodegradation reaction. The electrostatic attractions of MB and TiO_2 create the interface between them, as well as the pathway for charge transfer. The MB adsorption on TiO_2 surface can be described by Langmuir adsorption model [128-130]; an accelerated adsorption during the initial stage followed up by a deceleration stage and finally reaching the adsorption and releasing equilibrium. According to the Langmuir adsorption model, the coverage θ can be put like:

$$\theta = \frac{n_{ads}}{n_t} = \frac{KC}{1+KC} \quad \text{..... (2-11)}$$

Where n_t is the total number of adsorption sites, while K is the adsorption constant of MB.

Houas and Lachhe et al [127] reported in their study, four different concentrations of MB solution (5ppm, 15ppm, 25ppm, 30ppm) all reach the equilibrium adsorption within 1h in dark (Figure 2-6 white). A linear transform is also given (Figure 2-6 blue) to confirm its kinetic model.

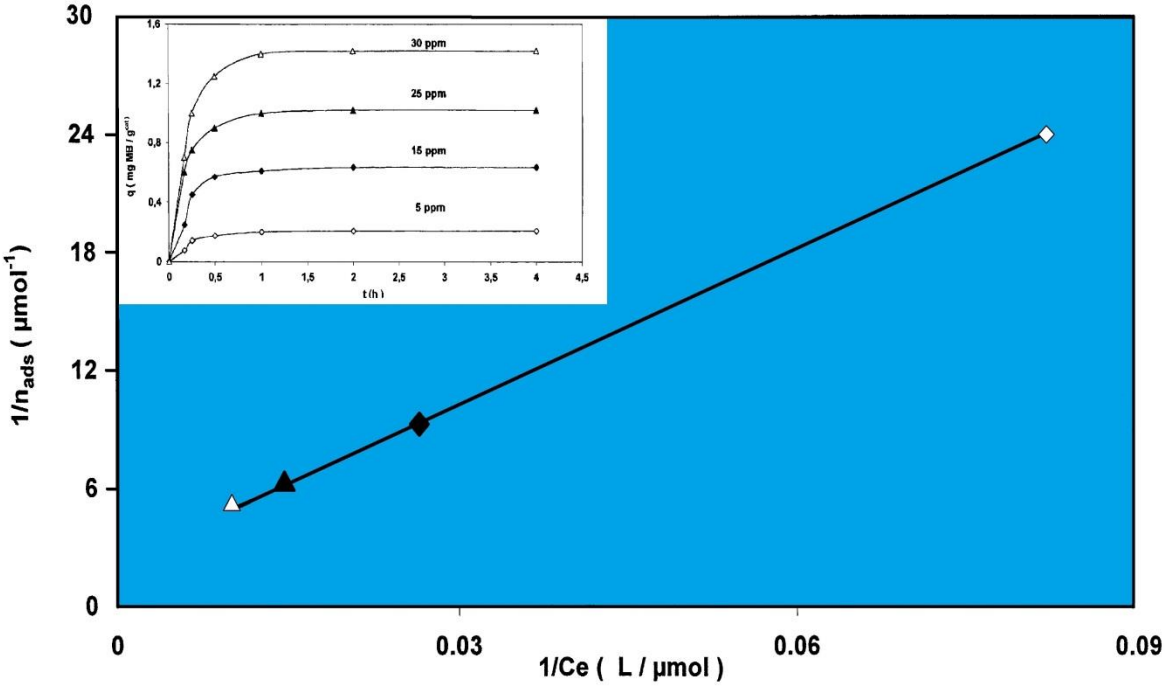

Figure 2-6 Kinetics of adsorption of MB in the dark, (blue) Langmuirian linear transform of the curve of MB adsorption in dark [127]

Disappearance of MB

The kinetic model of MB photodegradation has been proved to be a Langmuir–Hinshelwood model by previous studies [131-135], as the expression shows below:

$$r = \frac{dC}{dt} = \frac{kKC}{1+KC} \quad \text{..... (2-12)}$$

Where r is the degradation rate of MB, and *k* is the constant of degradation rate.

Thus, it is obvious that for MB diluted solutions, *KC*=1 and the reaction is of apparent first-order. After a certain concentration, the degradation rate starts to follow zero-order

kinetics. A noteworthy phenomenon has been reported by Demeestere and Visscher et al [136], that a pseudo-zeroth-order kinetic degradation can be observed for suspended TiO_2 mediated heterogeneous photodegradation of trichloroethylene in gas-phase.

2.5 Influence of Physical Parameters on MB Photodegradation

Initial Concentration (C_I) of MB

The kinetic of a MB photodegradation reaction follows a Langmuir–Hinshelwood mechanism where the initial reaction rates were found to be directly proportional to the C_I of MB. The degradation reaches its maximum rate when the zero-order kinetic is applied (Figure 2-7 a).

Mass of TiO_2 Photocatalyst

The degradation rates were found to be linearly proportional to the mass of TiO_2, as the Langmuir–Hinshelwood kinetic also applied for the catalyst loading (Figure 2-7 b). This can be understood by reviewing that: the reagent has to in direct contact onto the TiO_2 surface to bond pathways for the charge transfer. Additionally, those non-contacted TiO_2 might block the light source (especially TiO_2 nano particles), resulting in an even lower reaction efficiency.

Temperature

Unlike most catalytic chemical reactions which can be accelerated by using a higher reaction temperature. The increase of temperature enhances recombination of electrons and holes, as well as the desorption process of MB on the TiO_2 surface, resulting in loss of photocatalytic activity. However, at a very low temperature, the degradation rate of MB can be limited by the high apparent activation energy (Figure 2-7 c).

Wavelength of the Light Source

The absorbed photon energy has to equal or exceed the band gap of the TiO_2 (anatase of 3.2 electron volt, and 3.0 eV for rutile) to trigger a TiO_2 photodegradation reaction. According to Planck relation, this requires the wavelength of light source to be near or below 400 nm (UV-light) (Figure 2-7 d).

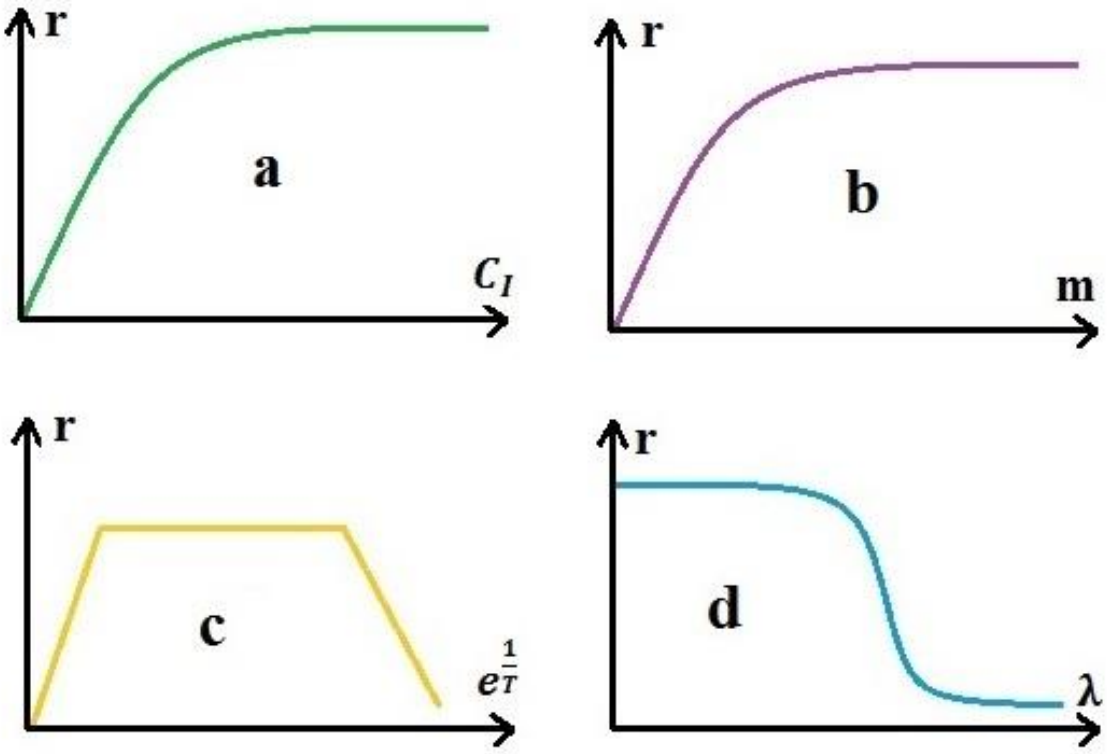

Figure 2-7 Influence of physical parameters for MB photodegradation (a) Concentration of MB (b) Mass of TiO_2 photocatalyst (c) Temperature (d) Wavelength of the light source

3. Modification to Promote Visible-Light Active TiO_2 Photocatalyst

As discussed in Chapter 2.1, anatase and rutile TiO_2 photocatalysts mainly absorb ultraviolet photons due to their large band gaps. This greatly limits the practical applications of pristine TiO_2 photocatalysts, because only 5% of solar spectrum consists of ultraviolet light. Therefore, as mentioned in Chapter 1, the development of visible light responsive TiO_2 has become one of the most important subjects in the field of photocatalysis. Different methods have been investigate in the past several decades, including metal and/or non-metal ion doping, surface deposition of noble metal, semiconductor coupling, photosensitization of photocatalysts. Among all those methods, the most representative and promising modifications are domestic doping and foreign coupling.

3.1 Metal Doping

From the point of view of crystallography, defects and impurities determine the photo-electrochemistry ability of a photocatalyst. The presence of metal ions in TiO_2 crystal would reduce electron and hole recombination, since charge carriers are more attracted to metal ions. For metal doped-TiO_2, the metal trapping center could capture electrons when the valence state of metal ion is higher than Ti^{4+}. On the other hand, when the valence state

of metal ion is lower than Ti^{4+}, holes would be captured. In addition, the presence of impurities lead to narrower band gaps than that of pristine TiO_2, Therefore, less photon energy is required for metal-doped TiO_2 to generate electron and hole pairs.

So far, researchers have synthesized and discussed almost every metal ion doped TiO_2 photocatalyst. The visible-light photocatalytic performance of metal elements – including alkali metals, alkaline earth metals, transition metals and rare earth metals – have all been tested through various means [137-159].

Alkali Metal/Alkaline Earth Metal Doping

Brezova et al [137] reported that several candidate metal ions, including Li^+, can be used as doping elements to enhance the photoactivity of TiO_2. According to their results, the sol-gel synthesized Li^+ doped-TiO_2 experienced a more significantly enhancement in Phenol photodegradation compared to Zn^{2+} or Cd^{2+} doped-TiO_2 prepared by same technique. Latter in 2001, Lopez et al [146] also obtained this kind of improvement in their study. They reported that the photodegradation efficiency of 2,4-Dinitroaniline can be improved by their sol-gel synthesized Li^+ and Rb^+ doped TiO_2. They also postulated that Li+ is the electron trapping center to capture holes. Potassium doped TiO_2 has also been reported to be more photoactive than the pure TiO_2. Morawski et al [148] reported a perovskite structure Potassium doped TiO_2 with a chemical formula $K_2Ti_4O_9$. The Phenol photocatalytic degradation experiment showed that $K_2Ti_4O_9$ contributes to photodegradation by generating more electrons and holes compared to pure TiO_2.

Alkaline earth metal doping has also been investigated. As Venkatachalam et al [153] reported that in their TiO_2 photodegradation of Bisphenol-A study, Mg^{2+} and Ba^{2+} doped nano-TiO_2 were found to be more efficient than the both the pure nano-TiO_2 and commercial TiO_2.

However, some studies have shown that the presence of Na^+ in TiO_2 lattice may damage the performance of the photocatalyst due to alkaline contamination from support subtract to photocatalyst [160, 161]. Local high concentration of dopant metal ions may serve as recombination centers for electrons and holes [162], which exists in all metal cation/cations doped TiO_2 photocatalysts.

Transition Metal Doping

Most transition metals have multiple potential oxidation states. Relying on this property, transition metals can greatly reduce the electron and hole recombination by efficiently serving as charge carrier trapping centers [163]. In general, compared to alkali or alkaline earth metals, the atomic radius of transition metals are more similar to that of TiO_2, making them more technically accessible into the crystal lattice of TiO_2 with inhibited migration [164].

Choi et al studied [79, 165, 166] nineteen transition metal ions as doping materials, including V^{3+} , V^{4+}, Cr^{3+}, Mn^{3+}, Fe^{3+}, Co^{3+}, Ni^{2+}, Zn^{2+}, Ga^{3+}, Zr^{4+}, Nb^{5+}, Mo^{5+}, Ru^{3+}, Rh^{3+}, Sn^{4+}, Sb^{5+}, Ta^{5+}, Re^{5+} and Os^{3+}. In their experiment, both the reduction of an electron accepter and oxidation of an electron donor were characterized via CCl_4 dechlorination, and $CHCl_3$ degradation respectively. Results showed that doping TiO_2 with V^{4+}, Mo^{5+}, Fe^{3+}, Ru^{3+}, Re^{5+}, Os^{3+} can remarkably increase the activity of TiO_2 photocatalyst. And there is an optimal doping concentration for each tested transition metal ion-doped TiO_2. A very rough approximation is also provided in their work: about 0.1-0.5wt.% would be a decent doping concentration in general.

Studies show that visible light photodegradation of organic compounds can be achieved by doping with transition metals such as Vanadium, Manganese, Cobalt, Tungsten, Chromium, Ferrum, and Nickel etc. Fuerte et al [167] and Anpo et al [162] studied the red shift in absorbance spectrum of several different kinds of transition metal doped TiO_2s. According to their results, besides the doping concentration, red shift rate in absorption varies from one doping transition metal to another. This shift, in order from greatest to smallest was found to be: Vanadium > Chromium> Manganese> Ferrum> Nickel. The red shift can be explain as the presence of transition metal ion in TiO_2 lattice which bridges the charge transfer from its own *d* electrons to the conductive band or valence band of TiO_2, so that less energy is required to activate the doped TiO_2 [168].

Rare earth metal and noble metal elements recently have drawn massive attention among all the transition metal elements. Doping with rare earth metals in the TiO_2 crystal,

especially Lanthanoids, can further promote the photocatalytic activity of TiO_2 by attracting the organic compound/compounds to the doped TiO_2 surface and forming Lewis acid/base complexes [169]. Regarding noble metals, they are highly resistant to corrosion and oxidation, which can greatly extend the lifetime of TiO_2 photocatalysts, since catalyst deactivation is a major threaten to the long term photoactivity of TiO_2. Currently, the manufacturing costs for rare earth metal or noble metal doped TiO_2 is the primary issue of concern to their practical application.

Overall, metal doped TiO_2 has distinctly shown its positive impacts on photocatalysis. However, doping with metals damages the thermal stability of TiO_2 semiconductors [170], and the doped metal ions sometimes inhabit the surface active sites of the photocatalysts [171].

3.2 Non-Metal Doping

Various Non-Metal elements, such as Nitrogen [172-178], Carbon [93, 179-182], Sulfur [178, 183-187], Boron [188-193], Phosphorous [194-197], Chlorine [198-200] and Fluorine [201-204], have frequently been reported in the past several years as a class of promising doping element to enhance and extend the photoactivity of pure TiO_2 to visible-light range. The mechanism of this absorbance in the visible light region brought on by non-metal ion doping can be explained with the help of the Figure 3-1.

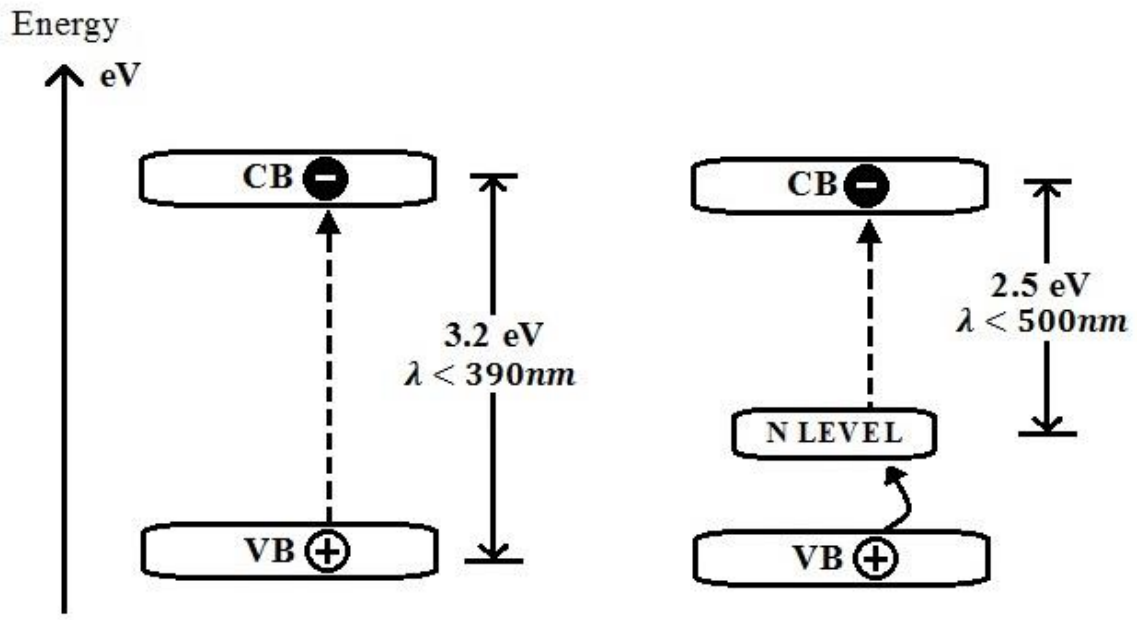

Figure 3-1 Mechanism of visible light absorption by in Nitrogen-doped TiO_2

In general, by doping with non-metal ions, the band gap of TiO_2 decreases since a "springboard" energy level between the valence band and conduction band contributes to the charge transfer [205]. Representatively, the most popular method for non-metal doping, Nitrogen doped TiO_2: the valence band of TiO_2 is primarily *O*-2*p* orbitals, while the conduction band consists of Ti-3*d* orbitals. Doping with Nitrogen ions brings an energy level in between them, and the orbitals of this energy level (*N*-2*p* orbitals) are very similar to the valence band. After the mid-way "springboard" energy level populates with electrons from the valence band, holes generated from the valence band, and the electrons can be pulled to the conduction band using less photon energy, which in this case, is about 2.5eV. That means the light-absorbance spectrum of this N-doped TiO_2 has been extend from 390nm (UV range) to 500nm (visible light range).

Among all the anion-doping materials, Carbon has been claimed to be another important candidate. Similar to Nitrogen, the introduced Carbon is *C*-2*p* orbitals. In the study conducted by Sakthivel et al [206], C-doped TiO_2 efficiently decomposed 4-Chlorophenol under visible light irradiation due to the red shift caused by Carbon substitutions at Oxygen sites inside the TiO_2 lattice. In some cases, the formation of carbonaceous species on the surface of C-doped TiO_2 has also been shown to promote the visible light response [207, 208].

Besides Nitrogen and Carbon doping, doping TiO_2 with Sulfur has been investigated as well. Studies showed some evidence of how the *S*-2*p* orbitals narrow the bang gap of TiO_2. However, these studies remain controversial in the academic community, as some researchers claimed that these results are possibly due to misleading characterization and are "partial" and “incomplete”[61, 123, 209].

The drawback of non-metal element doping is the poor thermal stability for doped non-metal ion inside the crystal lattice. A high temperature chemical process, annealing for instance, would reduce the concentration of the non-metal, leading to a low catalytic activity and poor visible light response of the doped TiO_2 photocatalyst [210]. Co-doping [178, 186, 190, 197, 210] with two or more metal/non-metal elements has been considered as one of several ways to overcome the drawbacks of metal or non-metal doped TiO_2 due to the synergetic effect of co-doped ions.

3.3 Semiconductor Coupling

Many researchers have reported their efforts on coupling narrow band gap semiconductor/semiconductors on the surface of TiO_2. Due to overlaps between the valence band, conduction band and band gap of two different semiconductors, this heterostructure system can effectively separate the photon-generated electrons and holes while hamper their recombination. The addition of a narrower band gap semiconductor can also extend the light response of this system to visible light region [211]. In this context, coupled TiO_2 heterostructures systems were considered to be a class of high visible light activity photocatalysts.

The basic mechanism of this technique is given below in Figure 3-2. The coupled semiconductor with a narrow band gap can be photo-active under visible light irradiation, the photon generated electrons from the conduction band of coupled semiconductor insert to the conduction band of in-activated TiO_2, while holes are left behind at the valence band of coupled semiconductor. The charge transfer process takes place at the interface between these two semiconductors, during which, active oxidative species generate and start to catalyze the reactants adsorbed on the coupled-TiO_2 [212, 213].

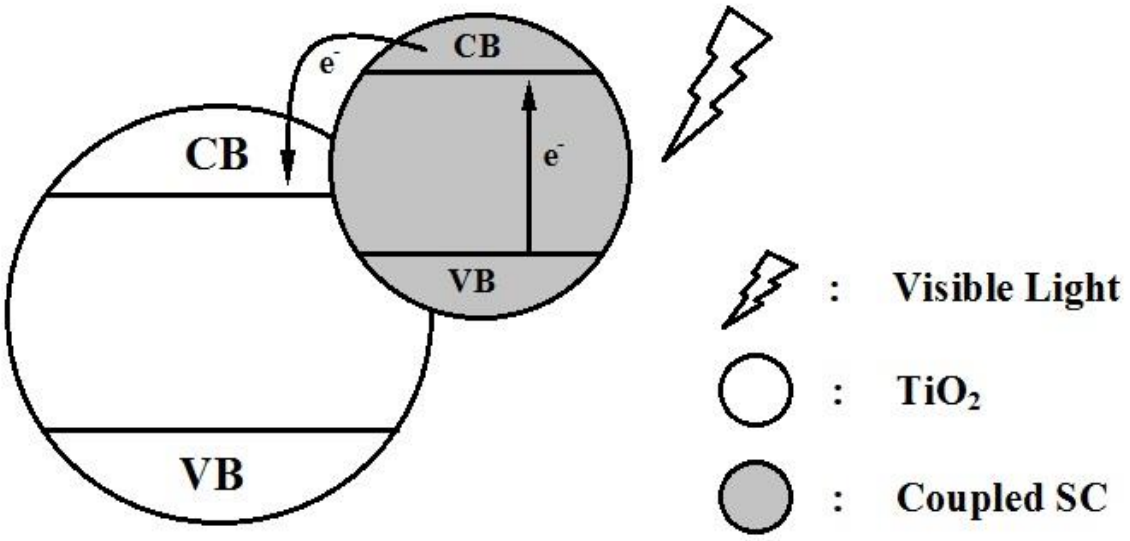

Figure 3-2 Visible light activation of TiO_2 coupled with a narrow band gap SC.

Spanhel et al [214] reported in 1987 the most important principle of selecting candidate coupling semiconductors: the band gap of coupling semiconductor must be shorter than the band gap of TiO_2 so that a visible-light response can be possibly achieved. Afterword, studies [212, 215] ascertained that the conduction band of coupled narrow band gap semiconductor has to be lower, while its valence band should be higher than which of TiO_2.

Various of coupling systems have been reported recently, such as CdS-TiO_2 [216-222], SnO_2-TiO_2 [223-225], SiO_2-TiO_2 [147, 226-228], WO_3-TiO_2 [17, 115, 229-233], Al_2O_3-TiO_2 [49, 226, 234-237], ZnO-TiO_2 [7, 93, 135, 238-240], ZnS-TiO_2 [241-243] and MoS_2-

TiO_2 [244-246] etc. Among them, the most in-depth studied material is CdS due to its deal band gap and energy levels.

Laurence et al [221] introduced layered CdS quantum dots to nanocrystalline TiO_2 electrodes by a self-assembly method. Characterization results showed that their TiO_2 can be effectively photo-sensitized via CdS coupling. A microemulsion-mediated solvothermal synthesis of nanoscale CdS-TiO_2 has been reported by Yu et al [222]. Using this method, a significant enhancement of visible-light absorbance was observed in their CdS-TiO_2 samples. Also, Yu's couple system was found to be more effective for the Methylene blue reduction under visible light irradiation compared to pure TiO_2. More importantly, electron paramagnetic resonance (EPR) spectrum identified the existence of Ti^{3+} in CdS-TiO_2. In contrast, no EPR signal of Ti^{3+} can be observed using the same characterization conditions and device for pure TiO_2 samples, which supports the idea of photo-generated electron injection from the CB of CdS to that of TiO_2.

Coupling with Transition Metal Dichalcogenides

Recent studies have demonstrated that nano-scaled transition metal dichalcogenides, or transition-metal disulfides (TMDs) with graphene-like mono or few layer structure experience strong anisotropy in many properties, especially electrical properties. The typical structure of TC_2, as shown in Figure 3-3 is a "sandwich" layered structure, where a layer of transition metal atoms is located hexagonally in between of two layers of chalcogen atoms. Inside the mono layer of TMD, transition metal atoms and the chalcogen

atoms are bonded to each other via wave-live covalent bonds, while the Van Der Waals force maintains the interaction along the surfaces of two "sandwich" layers.

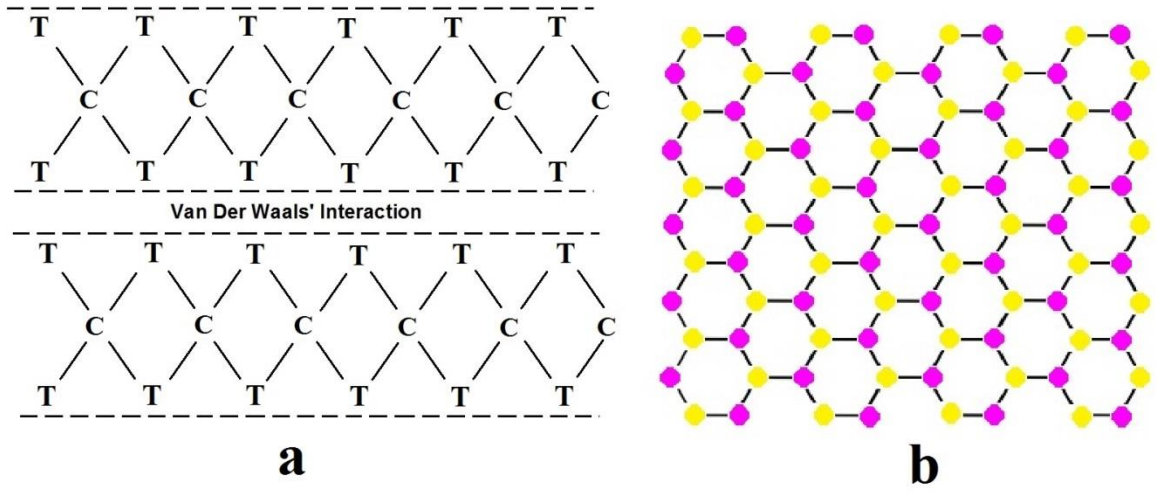

Figure 3-3 Sketch of the structure of typical TMD (a) X or Y-Axis view of two layers of TMD, each "T" stands for a transition metal atom while a "C" represents a chalcogen atom (b) Z-axis view of single layer of TMD, the yellow and magenta balls indicate the transition metal atoms and chalcogen atoms, respectively

TMDs such as MoS_2 and WS_2, have drawn considerable attention since they are easy to prepare at relatively low cost and have more photocorrosion resistance compared to conventional materials such as CdS and ZnO.

Ho et al [247] reported an in situ photo-reduction deposition synthesis of TiO_2 coupled MoS_2/WS_2 for enhanced visible-light photocatalysts. Figure 3-4 shows the experimental set up for the fabrication of MoS_2/WS_2-TiO_2. This method required a photochemical reactor with a high-pressure Mercury lamp as the light source. The nano-sized TiO_2 was suspended in the aqueous solution of $(NH_4)_2MoS_4/(NH_4)_2WS_4$, while Nitrogen gas was

continuously bubbled to the reaction system in order to protect the reactants from oxidation. The harvested MoS_2/WS_2-TiO_2 nano powder experienced a significant improvement in the visible-light decomposition of Methylene blue and 4-Chlorophenol, which they claimed, was due to the alerted energy levels of the conduction and valence band in the coupling systems.

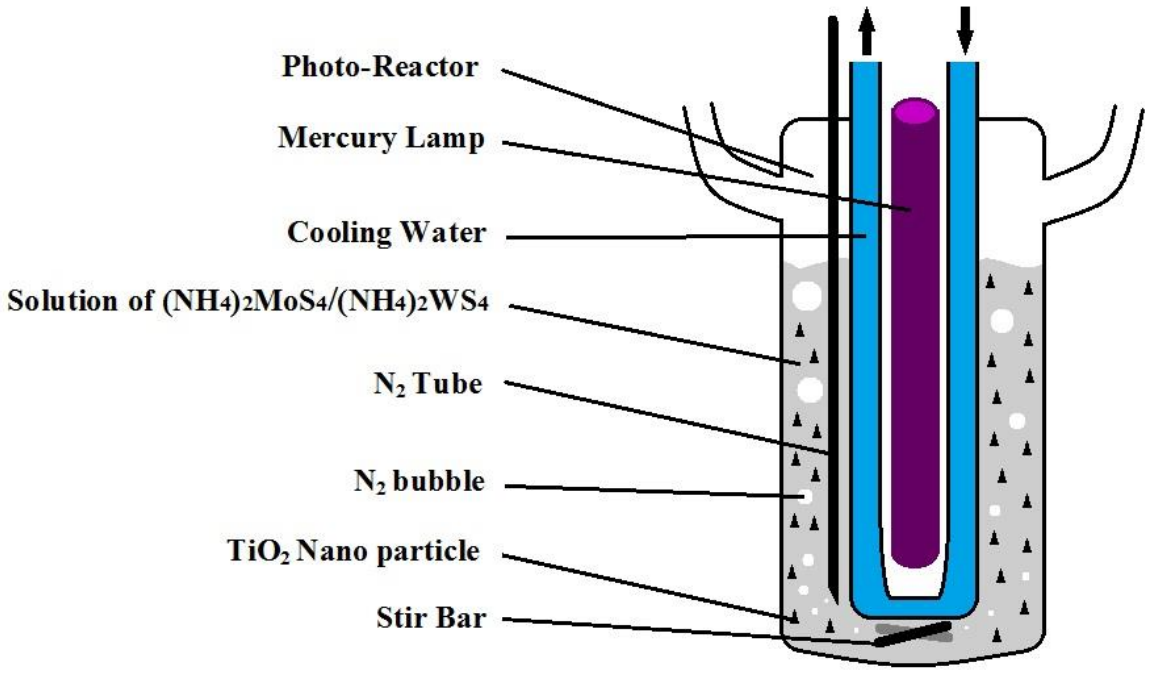

Figure 3-4 Sketch of the in situ photo-reduction deposition synthesis of TiO_2 coupled MoS_2/WS_2

An even more accessible method of semiconductor coupling has been investigated by Zhou et al [248], as they reported a visible-light active MoS_2-TiO_2 photocatalyst for hydrogen production and Rhodamine B photodegradation. In their study, a few-layer MoS_2 nanosheet-coated TiO_2 nanobelt hetero-photocatalyst system was synthesized by a hydrothermal reaction. The pre-synthesized TiO_2 nanobelts were suspended in the aqueous

solution of Thioacetamide (TAA) and Sodium Molybdate. After being heated in a Teflon-lined stainless steel autoclave at 200 ° C for 24 h, the outcome MoS_2-TiO_2 photocatalyst can be synthesized.

Figure 3-5 shows the characterization on the morphology of Zhou's samples, (a) is the scanning electron microscope (SEM) image of pure TiO_2 nanobelts. (b) is the SEM image of after-hydrothermal MoS_2-TiO_2 hetero-photocatalyst system, which was a remarkable evidence for its coupling heterostructure between two semiconductors. (c) and (d) are transmission electron microscopy (TEM) images of lattice fringes of MoS_2-TiO_2 that can further prove the chemical coupling between MoS_2 and TiO_2 can be achieved via a hydrothermal method.

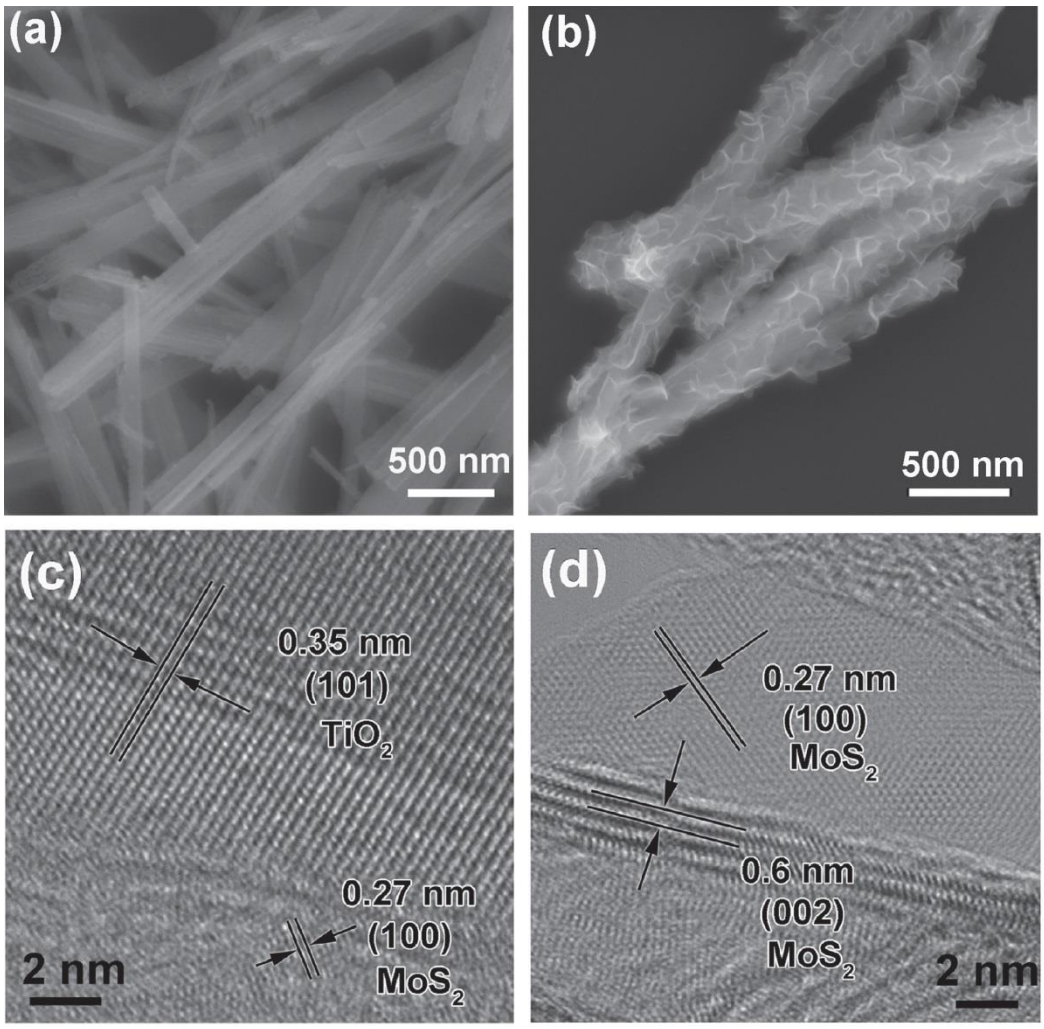

Figure 3-5 Morphology of TiO_2 nanobelts and MoS_2-TiO_2 coupling system (a) SEM images of pure TiO_2 nanobelts (b) SEM image of MoS_2-TiO_2 coupling system (c) and (d) TEM image of MoS_2-TiO_2 coupling system [248]

Brief Introduction of Nano Scaled VS_4

As already discussed in Chapter 1, VS_2 is a typical layered-structure TMD (Figure 3-6 a) which has been shown considerable attention recently due to its remarkable electrochemistry properties. However, the difficulties and complexities of VS_2 synthesis

make it necessary to seek other forms of vanadium sulfide minerals as substitutes in practical applications. Studies on some TMDs with S_2^{2-} dimer have shown that these materials have great potential in photochemistry and catalyst applications: Cattierite (CoS_2) is a possible electro-catalysis for Oxygen reduction [249]; while Vaesite (NiS_2), can be applied as Li batteries' anode material [250]. Thus, make the Vanadium Sulfide mineral with a fomular $V^{4+}(S_2^{2-})_2$, a very promising material in the field of electrochemistry.

The first recorded document of VS_4 was published in 1906 [251], when Hillebrasd found this Vanadium Sulfide mineral in Minaragra, Peru. VS_4 was named Patrónite in honor of Peruvian metallurgist Antenor Rizo-Patrón (1866–1948) who discovered the Vanadium ore in that area. In 1972, Kutoglu and Allmann [252] first reported the crystallography structure of VS_4 (article in German with English abs.): The VS_4 is a "linear-chain" compound (Figure 3-6 b) where a Vanadium center is octa-coordinated in between two four-sulfide-rectangulars.

The most recent work on VS_4 was carried out by Rout and Kim et al [253]. Single crystalline VS_4 nanostructures were successfully synthesized via a simple hydrothermal method, and a VS_4 based hybrid anode material for Li batteries with graphene oxide was synthesized. Material performance was demonstrated by initial discharge and charge capacities, which were found to be 1669 and 1105 mA h g^{-1}, respectively. And the VS_4 and Graphene Oxide hybrid showed good durability by remaining a high charge capacity of 954 mA h g^{-1} after underwent more than 100 charge and discharge cycles at 0.1 C. Also,

characterizations such as SEM, TEM and XRD were included in their report. This paper shows a great potential that VS_4 materials could have to apply in electrochemical field.

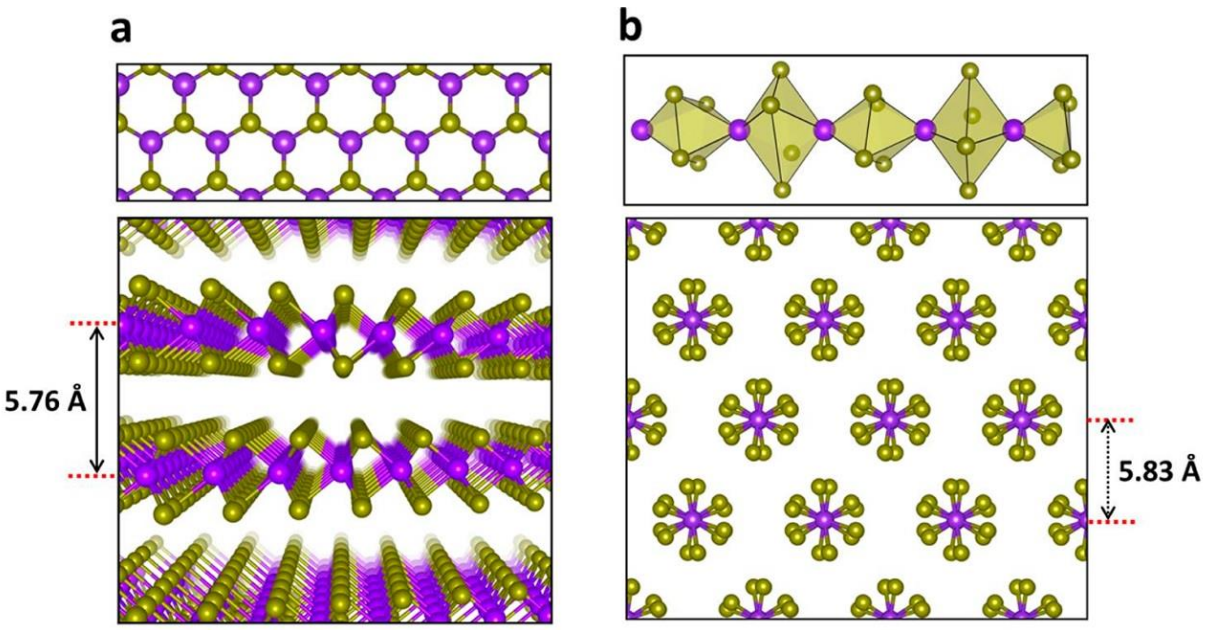

Figure 3-6 3-D geometries of VS_2 (a) and VS_4 (b); The purple balls are Vanadium atoms, while the golden balls are Sulfide atoms [253]

There have been scattered reports on VS_4 over the last 50 years, However, the difficulty of synthesize pure VS_4 greatly hinders the researchers to study it systematically. The nonstoichiometric phases of Vanadium Sulfides with various different oxidation states are so difficult to limited by controlling the sulfurization process during synthesis [254], and separating VS_X from existing VS_4 is also intractability in practice [255, 256].

4. Experimental Section

4.1 Synthesis

Materials

Sodium Orthovanadate (Na_3VO_4, 99.8%), Thioacetamide (TAA, C_2H_5NS ≥99.0%), Titanium (IV) Oxide nanopowder (P25, ≥99.5%) and Methylene blue (MB, ≥82%) were commercially available from Sigma-Aldrich Co. LLC. All reagents were conducted using double-deionized water and used as received without further purification.

Preparation of VS_4 Nano Materials

In a typical experiment, 552 mg Sodium Orthovanadate (Na_3VO_4) and 1.125 g Thioacetamide (C_2H_5NS) were dissolved with 30 mL double deionized water and stirred vigorously for 5 minutes to dissolve all reagents, then the contents were transferred to a Teflon-lined stainless-steel autoclave and heated in an electric oven at 160 ℃ for 24 hours. Black precipitate was finally collected by centrifugation at 10K rpm and washed 5 times with double deionized water. The wet black product was re-dispersed in 15 mL double deionized water. The above dispersion was sonicated in an ice bath for 1 hour. The resultant black VS_4 was harvested after centrifugation and freeze dried at -40 ° C for 12

hours. Notice that different reaction parameters such as temperature or time lead to different morphologies as listed in Table 4-1.

Synthesis of VS_4-on-TiO_2

The process of growing nano VS_4 discs on nano TiO_2 heterostructures (6 wt.% of VS_4) is described as follows. Typically, 6 mg VS_4 nanodiscs and 94 mg of P25 were dissolved with 25 mL of double deionized water in a 30 mL vial. Then this dispersion was heated with a hot-plate magnetic-stirrer at 100 ° C and bubbled with Nitrogen gas for 3 hours. The desired nano VS_4-on-TiO_2 samples were obtained after centrifugation and freeze dried at -40 ° C for 12 hours. Different loadings of VS_4-on-P25 have been synthesized via the same method (1wt.%, 3wt.%, 10wt.%, 20wt.%). The influence of photocatalytic activities for different loading of VS_4-on-P25 will be discussed in the following Chapter 5

Table 4-1Various VS_4 products obtained by different hydrothermal parameter

Parameters / Morphology	Reaction Time	Reaction Temperature	Reactants Concentration	Comment
Nanodiscs	24 h	160 °C	552 mg Na_3VO_4 + 1.125 g C_2H_5NS + 30 mL H_2O	Figure 5-1
Micro-Spheres	36 h/48 h	160 °C	552 mg Na_3VO_4 + 1.125 g C_2H_5NS + 30 mL H_2O	Figure 5-2
Nanorings	24 h	200 °C	46 mg Na_3VO_4 + 120 mg C_2H_5NS + 30 mL H_2O	Figure 5-3
Micro-Cluster	36 h	200 °C	46 mg Na_3VO_4 + 120 mg C_2H_5NS + 30 mL H_2O	Figure 5-4
Micro balls and rods	36 h	200 °C	3.312 g Na_3VO_4 + 6.65 g C_2H_5NS + 30 mL H_2O	Figure 5-5

4.2 Characterizations

Field-emission scanning electron microscopy (FESEM, Zeiss ULTRA Plus; 10 kV acceleration voltage), transmission electron microscopy (TEM, JEOL 2010F; 200 kV acceleration voltage), X-ray diffraction (XRD, Bruker AXS D8 Advance), and Raman spectroscopy (Bruker SENTERRA; 532 nm 20 mW laser) were employed to determine the morphologies, and crystal structures of materials.

Material performance was determined by the photocatalytic degradation of MB under UV light irradiation (500 W Mercury lamp, Beijing CEL Sci-Tech Co., Ltd). 30 mg of photocatalyst was added to a 40 mL MB aqueous solution (1.56×10^{-3} M) and stirred in dark for 30 min to achieve adsorption–desorption equilibrium, during which, 1 mL sample solution were drawn at 10, 20, and 30 min. Then the UV lamp was applied, under irradiation, 1 mL sample solutions were drawn at 1, 2, 3, 4, 5, 10, 15, 20, and 30 min. After diluting 4-folds and centrifuging to remove the photocatalyst, the concentration of MB was obtained using a UV-Vis photospectrometer (Fischer Scientific, GENESYS 10S). The absorbance was measured at the characteristic MB peak (664 nm). Diffuse reflectance absorption data of materials were obtained using a diffuse reflectance UV-Vis recording spectrophotometer (Shimadzu Corporation UV-2501PC).

5. Results and Discussion

5.1 Scanning Electron Microscopy

SEM was used to investigate the morphology and microstructure of the synthesized VS_4 materials. As it discussed in Chapter 4.1, five different VS_4 materials have been developed in this study. Among them, two are in nano-scale and the rest three are in micro size.

Nanodiscs

Figure 5-1 (a) demonstrates the uniformly distributed VS_4 nano discs. The prepared nanodiscs were synthesized at 160℃ for 24 hours, and the initial concentrations of Na_3VO_4 and C_2H_5NS (TAA) are 0.1 mol/L and 0.5 mol/L, respectively. A single prepared nanodisc is approximately 100 to 200 nm in diameter with a thickness of 10 to 20 nm (Figure 5-1 b, c). Self-assembly is common, as some nanodiscs self-assembled to form microspheres during the synthesis. However, most of the particles are remain in the nano-scale with no more than three self-assembled discs (Figure 5-1 d).

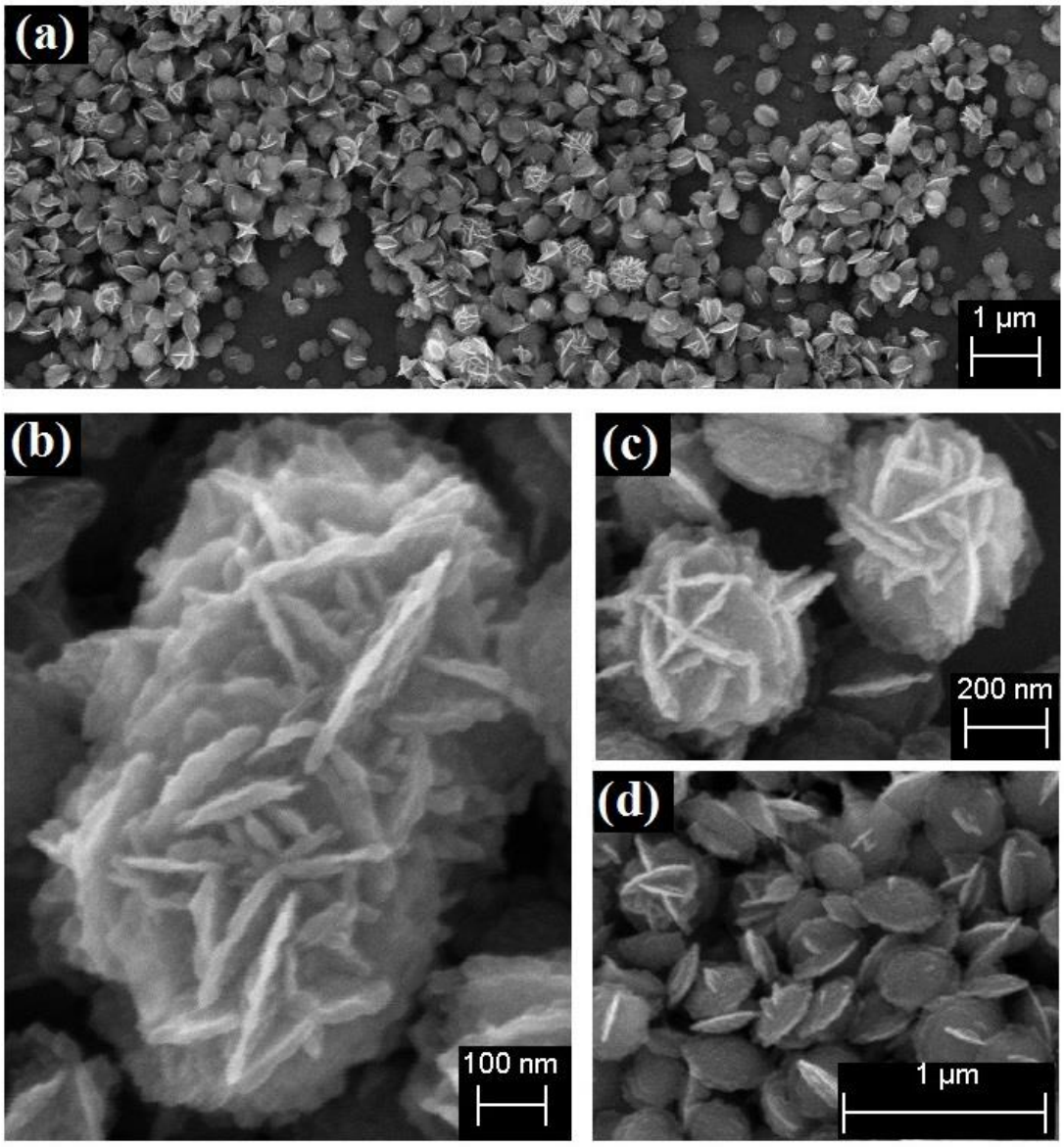

Figure 5-1 SEM images of VS_4 nanodiscs (a) uniformly distributed VS_4 nanodiscs; (b) (c) self-assembly of VS_4 nanodiscs; (d) mono or limited self-assembled VS_4 nanodiscs

Micro-Spheres

A time study was applied to investigate the growth of VS_4 nano material under different reaction time (36 and 48 hours). This demonstrates that the self-assembly of the nanodiscs

was more pronounced as the reaction time increases: the size of single nanodiscs remains the same regardless of the different reaction times (Figure 5-2 a, c). However, most of the nanodiscs self-assembled to form micro-spheres. A similar phenomenon has been reported by Zhou et al [248], where in their study, another kind of nano TMD (MoS_2) micro-spheres (Figure 5-2 e) have been hydrothermally synthesized using Sodium Molybdate ($Na_2MoO_4 \cdot 2H_2O$) and TAA as the precursors. Their time study also indicates that the size of micro-spheres increases with the reaction time due to the self-assembly process. The average diameter of the VS_4 micro-spheres is 1 to 2 um for the 36 hours group, while this number becomes inconclusive for the 48 hours group due to the presence of large clusters that are over 10 ums in diameter. (Figure 5-2 b, d)

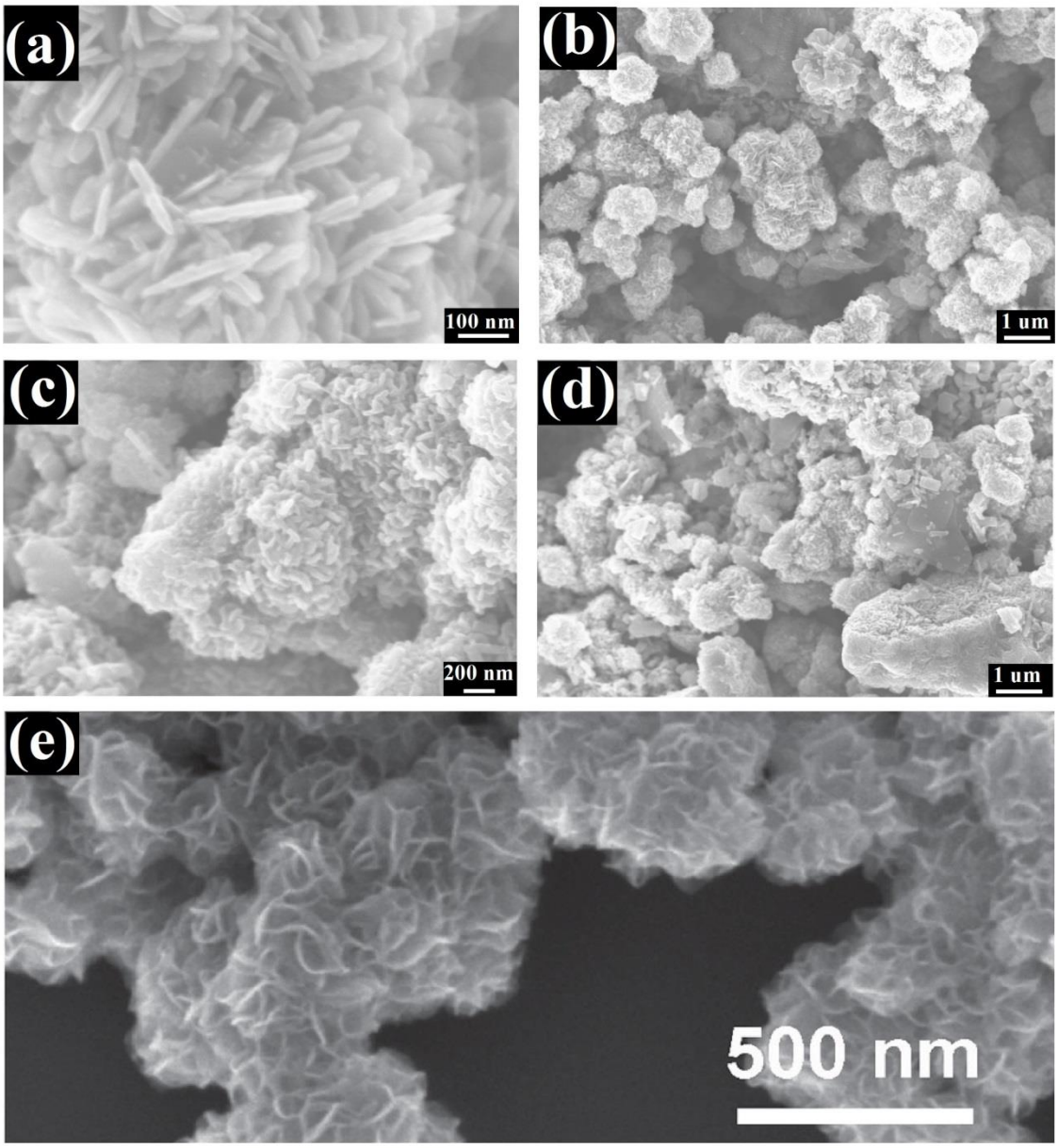

Figure 5-2 SEM images of VS_4 Micro-Spheres (a) (c) VS_4 Micro-Sphere after 36 hours reaction time; (b) (d) VS_4 Micro-Sphere after 48 hours reaction time; (e) MoS_2 Micro-Sphere [248]

Nanorings

The nanoring structures were obtained by a hydrothermal reaction at 200℃, which is the maximal temperature for this reaction system since the melting point of Teflon-lined chamber is 220℃. The initial concentrations of both two precursors are 8.3×10^{-3} mol/L (Na_3VO_4) and 5.3×10^{-2} mol/L (TAA). For a typical nanoring structure, several small nanoparticles comprise a ring that has inside and outside diameters of 100 and 200 nm, respectively (Figure 5-3 a). The thickness of these nanorings is not homogenous, and usually the thinnest part of a nanoring can be observed at the connection points of two small nanoparticles (Figure 5-3 a, b). In general, this ring-structured nano VS_4 is soundly uniform in size and shape. However, due to a higher surface energy caused by its large surface area, the nanoring structure undergo more favorable self-assembly compared to the nanodiscs (Figure 5-3 c).

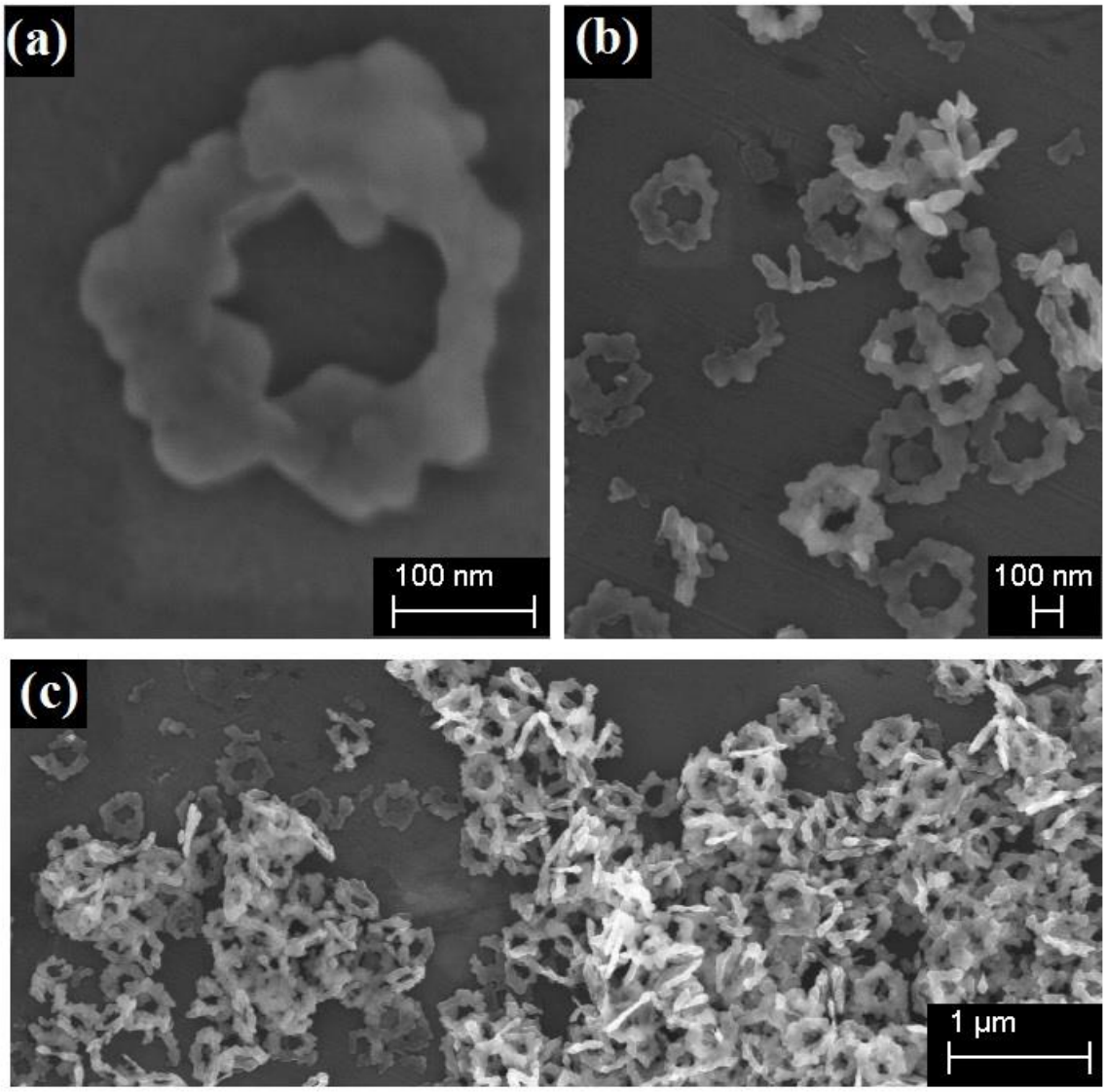

Figure 5-3 SEM images of VS_4 nanorings at different magnifications (a) (b)mono VS_4 nanoring consisted with small VS_4 nanoparticles; (c) self-assembly of VS_4 nanorings

Micro-Cluster

A time study has also been applied to investigate the growth of nanorings with a longer reaction time (36h). This time study shows that VS_4 nanoparticles have a strong self-assembly tendency under this reaction condition due to their specific surface area and large

surface energy. However, the size of a single nanoparticle would not be affected by reaction time. For one nanoparticle, the size remains at a diameter around 50 nm (Figure 5-4 a,b), Although a few nanorings still can be found under SEM, most of them self-assembled into micro-scale clusters (Figure 5-4 b,c).

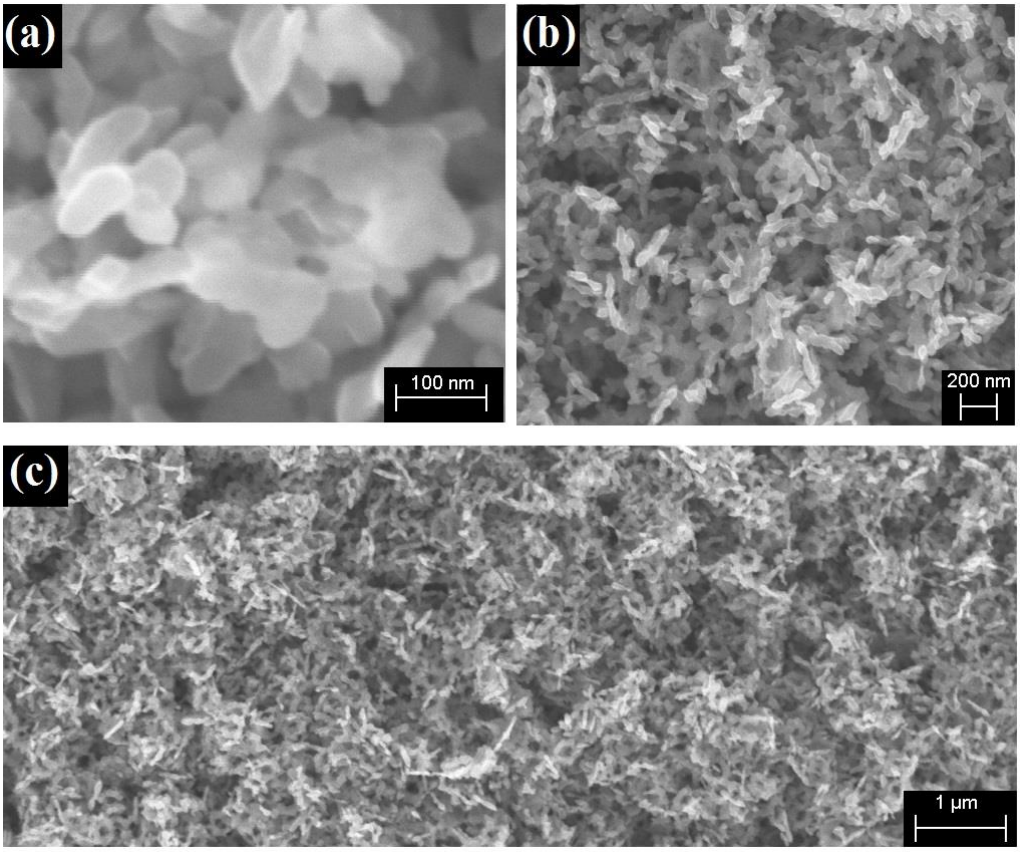

Figure 5-4 SEM images of VS_4 Micro-Clusters at different magnifications

Micro Balls and Rods

The limitation initial concentrations of this reaction are 0.6 mol/L and 3 mol/L for Na_3VO_4 and TAA, respectively. This is due to the formation of H_2S gas as a part of the side reaction, overloading of the two precursors could increase the risk of autoclave leaking or explosion. At this high concentration, the synthesized material is no longer in nano-scale: Micro balls and rod structures can be obtained as shown by SEM imaging (Figure 5-5). The Micro balls are made up with petal-like nanoparticles which are around 100 nm wide and 200nm in length as the core, surrounding by nano rods which are 50nm in diameter and several microns long (Figure 5-5 a, b). ThEse micro balls and rods are uniformly distributed, and the balls are mostly around 2 um in diameter and show a very limited degree of self-assembly between two or more micro balls (Figure 5-5 c, d).

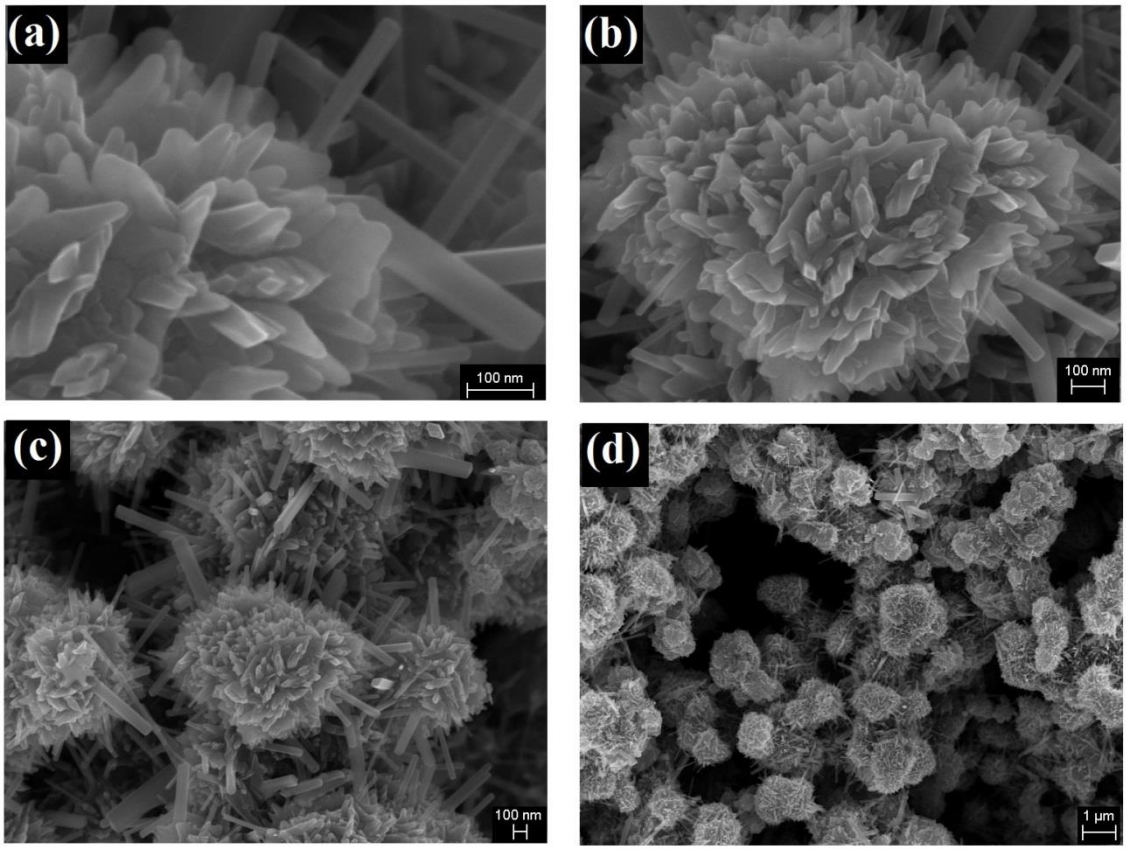

Figure 5-5 SEM images of VS_4 Micro balls and rods at different magnifications

According to the experiment results of the synthesis of VS_4-on-P25, it suggested that the nanodisc structure VS_4 is the most suitable material to grow onto P25 surface due to its relatively low surface energy compared to the size. Thus, staring from Chapter 5.2, all the VS_4 materials that conducted with VS4-on-P25 are VS_4 nanodiscs.

5.2 High-Resolution Transmission Electron Microscopy

The HRTEM images of pure VS_4 nanodiscs and VS_4-on-P25 are shown in Figure 5-6. The *d*-spacing of prepared nanodiscs is approximately 0.56nm, which corresponds to that of the (110) plane of monoclinic phase of VS_4 [PDF No. 072-1294, *d* (110) = 0.56 nm]. Long-range ordering of the VS_4 crystals was observed both in Figure 5-6 (a) and (b). Figure 5-6 (b) further verifies the growth of nanoscale VS_4-on-P25. However, compared to Rout and Kim et al [253] study on VS_4, the tested VS_4 nanodiscs show less in crystal regulation.

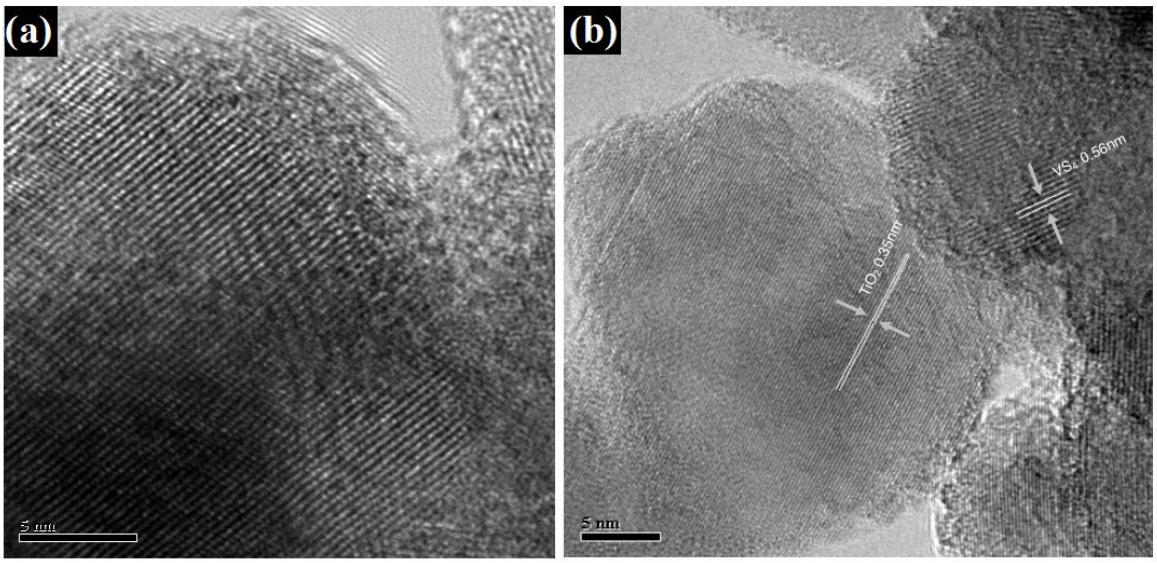

Figure 5-6 HRTEM images of (a) the VS_4 nanodiscs. (b) The VS_4-on-P25, ribbon showing TiO_2 lattice spacing of 0.35 nm in the (101) plane of anatase TiO_2[257]; and the VS_4 lattice spacing of 0.56 nm corresponding to the (110) plane

5.3 X-ray Diffraction

XRD was conducted using Cu K α radiation with a wavelength of 1.54 °A. Figure 5-7 shows typical XRD patterns of VS_4 nanodiscs using JCPDS No. 072-1294 as reference.

Characteristic peaks at each degree are marked in the figure. Compared to the standard JCPDS No. 072-1294, the XRD patterns of tested VS_4 sample have greater noise levels, and two or three characteristic peaks cannot match the reference, which offers more support to the cause of the less crystallinity TEM image in Chapter 5.2.

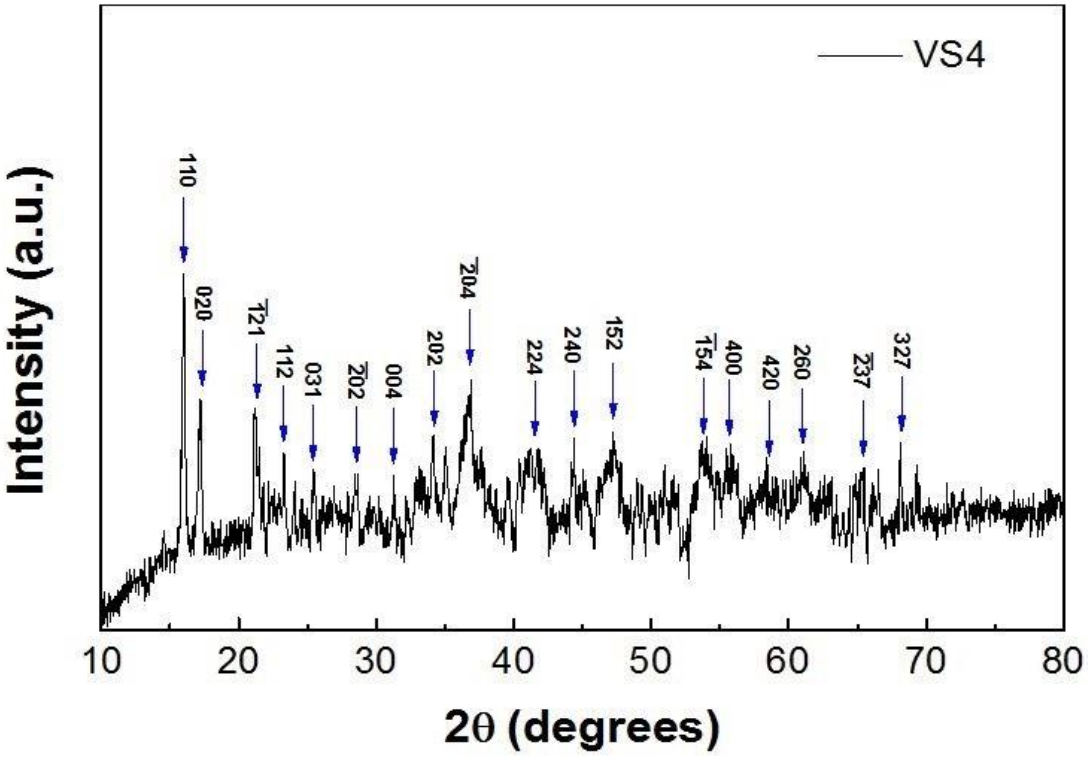

Figure 5-7 XRD pattern of VS_4. Refrence from known monoclinic VS_4 [JCPDS No. 072-1294]

The XRD spectra of pure P25 and 6 wt.% VS_4-on-P25 are also given in this study. For pure P25 samples, characteristic peaks of anatase phase TiO_2 at 25.5°, 38.0°, 48.2°, 54.1°, and 55.2° are marked in the Figure 5-8 as "A". While the peaks of a rutile phase TiO_2, as indicated by the characteristic peaks at 27.4°, 36.3° and 69.0°, are marked in the Figure 5-8 as "R"[258]. A typical XRD pattern of 6 wt.% VS_4-on-P25 shows that the VS_4 phase is not

readily detected in the composite due to the low loading of VS_4, which is in agreement with some literatures, that the XRD would failed to detect at this low degree of loading [257, 259].

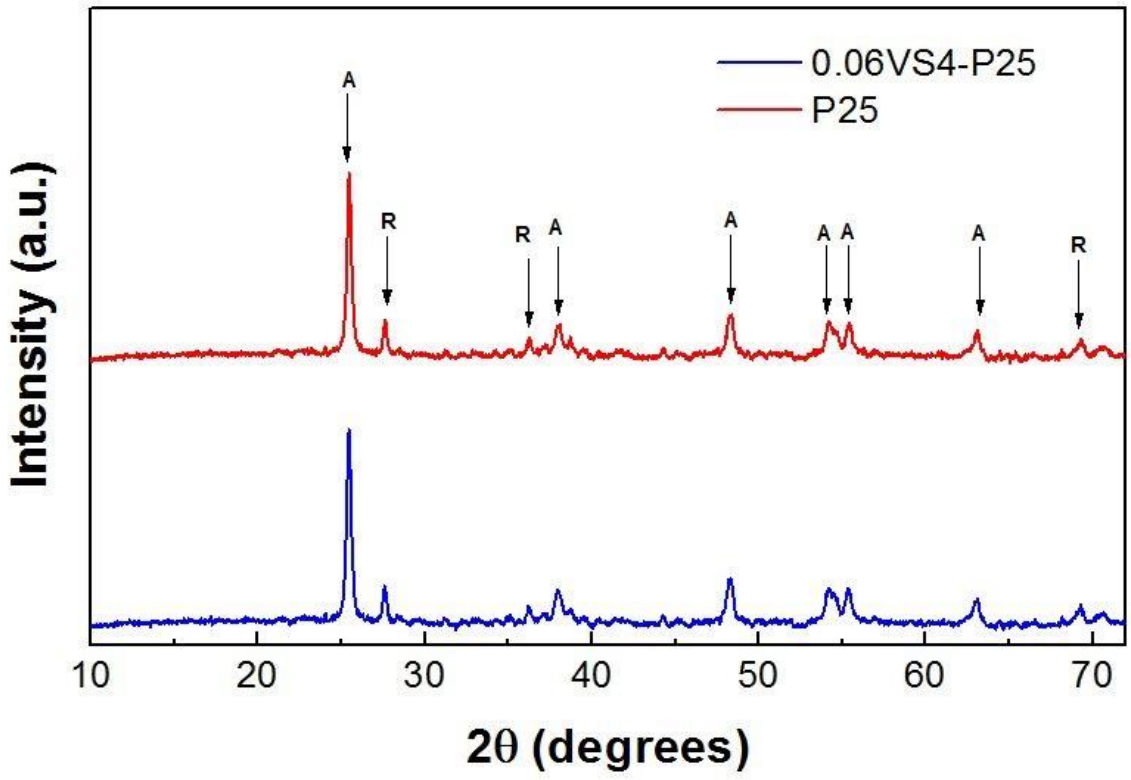

Figure 5-8 XRD pattern of VS_4-on-P25 and P25

5.4 Raman Spectroscopy

The Raman spectrum of VS_4 nanodiscs is also reported in this article. However, no previous work has ever been published on this characterization of VS_4 nanomaterials.

Moreover, the XRD data already shows the insufficient crystallinity and/or fineness on this test VS_4 sample. Thus, the Raman spectroscopy result can be only provided as rough approximations.

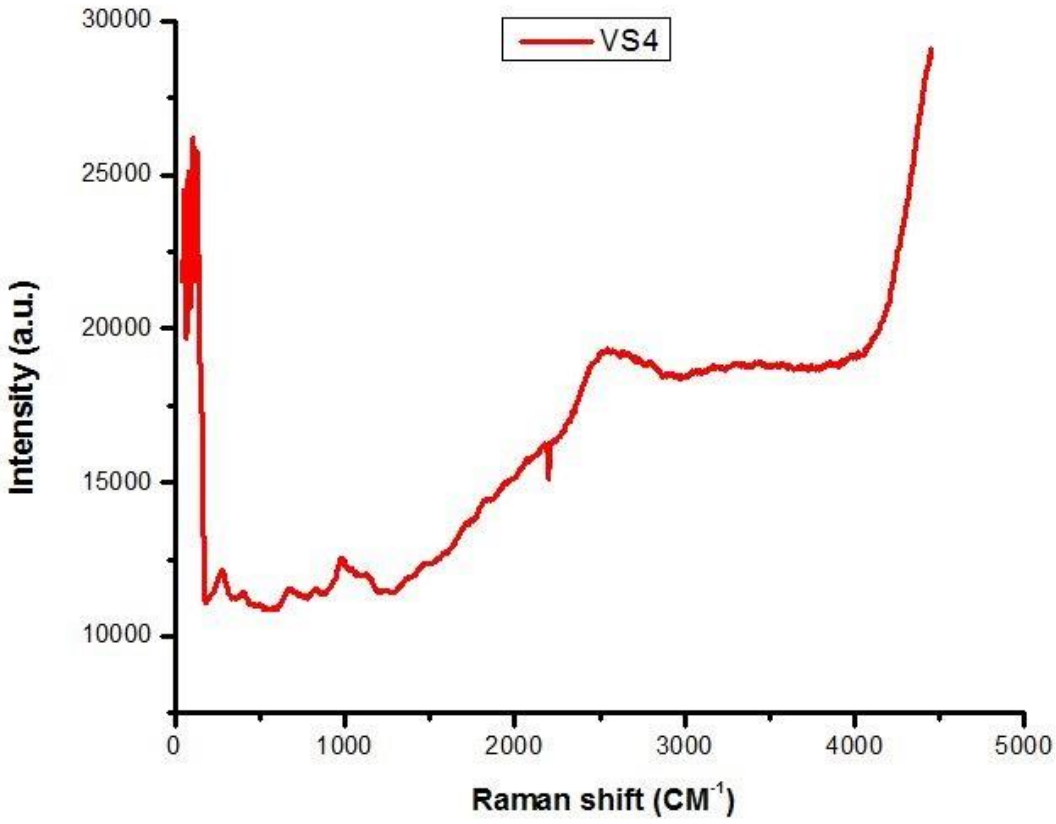

Figure 5-9 Raman spectroscopy of VS_4 nanodiscs

5.5 Ultraviolet–Visible Spectroscopy

The photodegradation activity of pure P25 and VS_4-on-TiO_2 was determined via UV decomposition of Methylene Blue. The equipment and procedures of this test have already been discussed in Chapter 4.2.

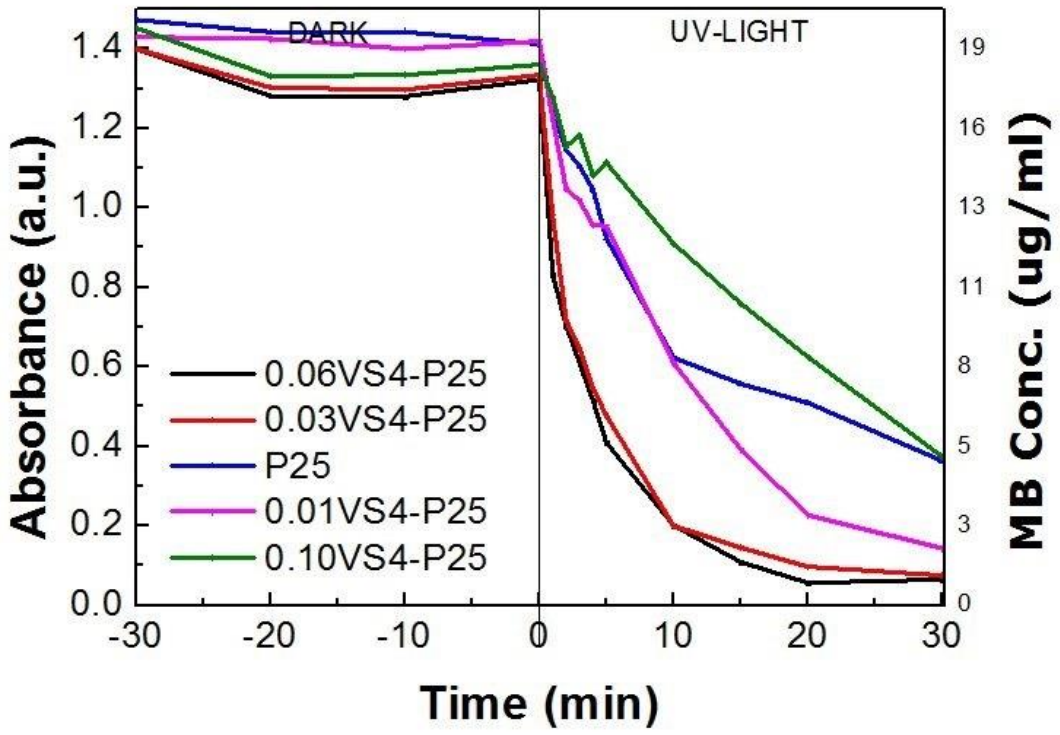

Figure 5-10 Photodegradation of Methylene blue under UV irradiation, comparing the performance of commercial P25 and 4 different VS4-on-P25s (1wt.%, 3wt.%, 6wt.%,10wt.%)

Figure 5-10 shows the photodegradation of MB over 30 minutes' of UV irradiation using 4 different VS_4-on-P25s (1wt.%, 3wt.%, 6wt.%, 10wt.%) and pure P25. The degradation curves of MB on different catalysts are typically first order kinetics. Thus, lists in Table 5-1, are the simple calculations of the degradation rate via the equation:

$$k = -\frac{ln\frac{C}{C_I}}{T} \quad \text{..... (5-1)}$$

In which C is the final concentration of MB and C_I is the initial concentration of MB, T is the reaction time and k is the degradation constant.

Table 5-1 Rate constant calculations for data obtained from Figure 5-10

Sample	MB initial concentration C_I (μg/mL)	MB final concentration C (μg/mL)	degradation constant k (min^{-1})	k/k_{P25}
P25	18.8	4.81	0.045	1.00
1wt.% VS_4-on-P25	18.9	1.87	0.077	1.71
3wt.% VS_4-on-P25	17.7	1.07	0.094	2.09
6wt.% VS_4-on-P25	17.6	0.8	0.103	2.29
10wt.% VS_4-on-P25	18.1	5.06	0.042	0.93

At 1wt.%, 3wt.%, and 6wt.% VS_4-on-P25 outperforms pure P25 in MB photodegradation. Quantitative measurements are given in Table 5.1, the highest degradation rate constant is provided by 6wt.% VS_4-on-P25, 0.094 min^{-1}, which is 2.29 times higher than that of pure P25's 0.045 min^{-1}. The 1wt.% and 3wt.% VS_4-on-P25 offer the improvements of 71% and 109%, respectively. Three loadings of VS_4-on-P25 samples are superior to pure P25 when the residual MB concentration is lower than 8ug/ml. These improvements can be attributed to the heterostructure of the VS_4-on-P25. The VS_4 crystalline nanostructure accelerates

charge transfer, resulting in lower electron-hole recombination rates compared to pure TiO_2 nanoparticles.

Several readings with fluctuations from 0 to 10 minutes (under UV irradiation) were obtained within 10wt.% VS_4-on-P25. Also, the rate constant of 10wt.% VS_4-on-P25 can be mathematical derived by dividing that of P25, k (P25)=0.045 (min^{-1}) and k (10wt.% VS_4-on-P25)=0.042 (min^{-1}), this quantitative measure shows that the 10wt.% VS_4-on-P25 actually performs worse that pure P25 by 7%.

To better understand how different loadings of VS_4 impact the heterostructure's photocatalytic performance, a same MB degradation study has carried out using 20wt.% VS_4-on-P25 (30 mg in total, 6 mg VS_4 contains) and pure VS_4 (6 mg). Figure 5-11 shows the results of MB degradation over 30 minutes storage in dark and 30 minutes' under UV irradiation. Significant fluctuations can be found with both 20wt.% VS_4-on-P25 and pure VS_4 samples. High but unstable absorbance for MB can be detected within the first 30 min in dark experiment until the dye-catalyst system reaches adsorption–desorption equilibrium.

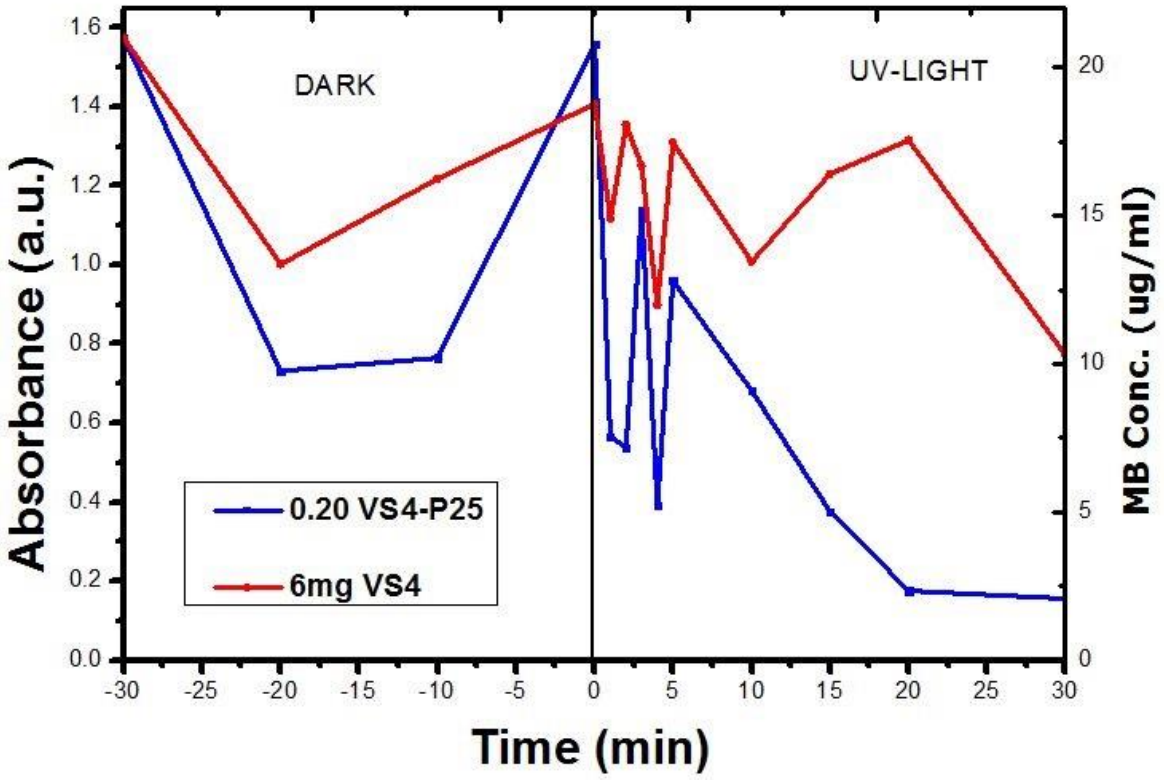

Figure 5-11 Photodegradation of Methylene blue under UV irradiation, comparing the performance of pure VS_4, and 20wt.% VS_4-on-P25

Also, the fluctuations on photodegradation curves under UV irradiation can be ascribed to the temporarily combination between MB and VS_4: when MB is attached on the surface of VS_4 or VS_4-on-P25, the extended interface between them allows an acceleration of the photodegradation process by bridging the charge transfer. As a result, the MB concentration of the solution fluctuates greatly contributed by both photodegradation and adsorption. For the 20wt.% VS_4-on-P25 group, after 5 min UV irradiation, MB photodegradation starts to predominate over adsorption, lead to the appearance of a first

order kinetic in Figure 5-11 (blue curve). Due to the relatively large VS_4 surface area and the absent of TiO_2 compared to VS_4-on-P25s, pure VS_4 experiences a violent absorb-release process under UV irradiation which is reflected in Figure 5-11 (red curve): the wild fluctuations last over 20 min.

5.6 Diffuse Reflectance UV-Vis Spectroscopy

A diffuse-reflectance UV-Vis recording spectrophotometer was applied to detect the light absorption for different materials. Figure 5-12 shows the light absorption spectrum of P25, 1 wt.% VS_4-on-P25, 6 wt.% VS_4-on-P25, and VS_4 samples. Pure P25 (red curve) follows the pattern of a typical TiO2's absorption spectrum: the TiO_2 material stops responding when the incoming light is in visible-light range (400 nm). Compared to P25, both 1 wt.% VS_4-on-P25 and 6 wt.% VS_4-on-P25 extends their absorptions into the visible range, especially the critical range in between 400 nm and 500 nm due to the strong UV and visible-light absorption ability of pure VS_4 (green curve).

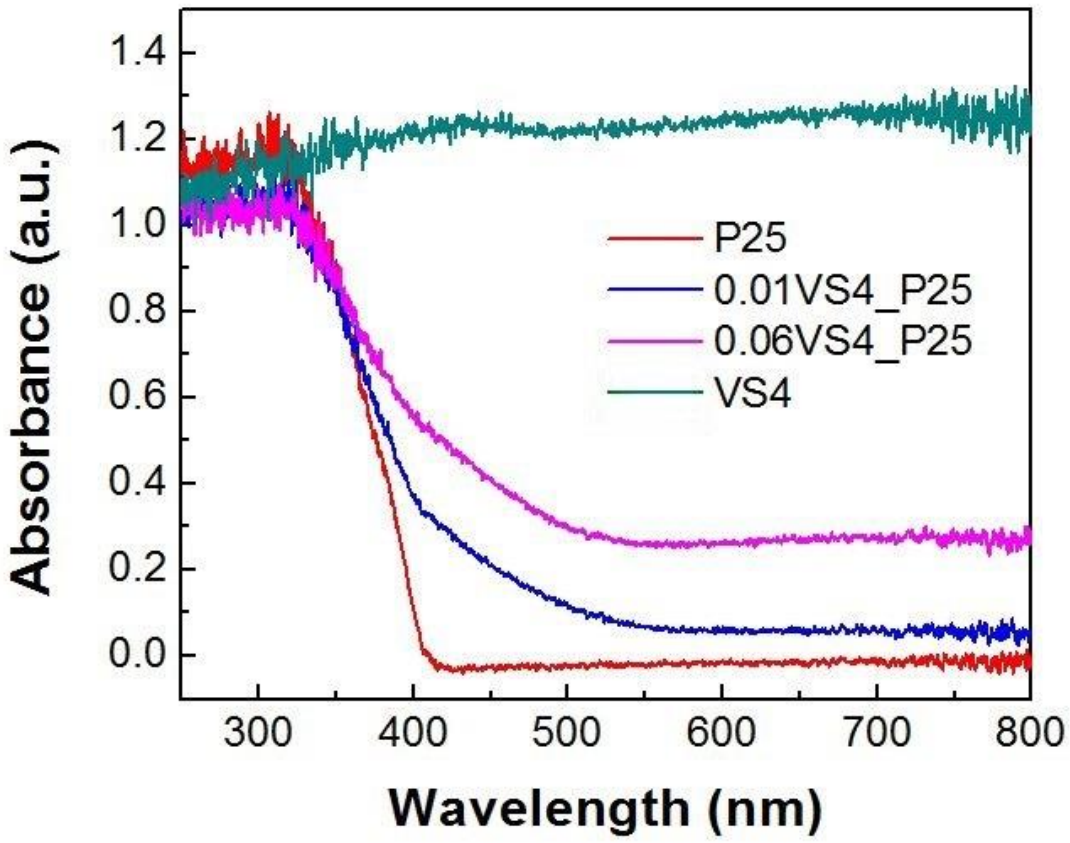

Figure 5-12 Light absorption spectrum of P25, 1 wt.% VS_4-on-P25, 6 wt.% VS_4-on-P25 and pure VS_4

A Tauc plot (Figure 5-13) can be generated after a Kubelka-Munk transformation on light absorption data [260, 261]. In this Tauc plot, (Y) axis represents Kubelka–Munk function $[F(R_\infty)hv]^{\frac{1}{2}}$, which approximately equals to $ahv^{\frac{1}{2}}$ (a is the material absorption coefficient). The horizontal (X) axis represents photon energy hv. Extrapolating tangents (black lines) established from the linear region of the curve to the abscissa, sketchy-calculated band gaps for P25. 1 wt.% VS_4-on-P25, and 6 wt.% VS_4-on-P25 can be found at 3.0 eV, 2.5 eV, and 2.1 eV respectively. Therefore, coupling VS_4 on TiO_2 can increase the

charge generation efficiency by extending TiO_2's light absorption spectrum to visible light range. Consequently, this heterostructured photocatalyst can reduce the recombination rate of photogenerated electron-hole pairs, results in a superior photocatalytic activity compared to pure TiO_2. It is worth noting that due to the lack of data on VS_4's absorption coefficient, all the Kubelka-Munk transformations of VS_4-on-P25 materials are acquired by using the absorption coefficient of TiO_2, which may lead to the lessening of results.

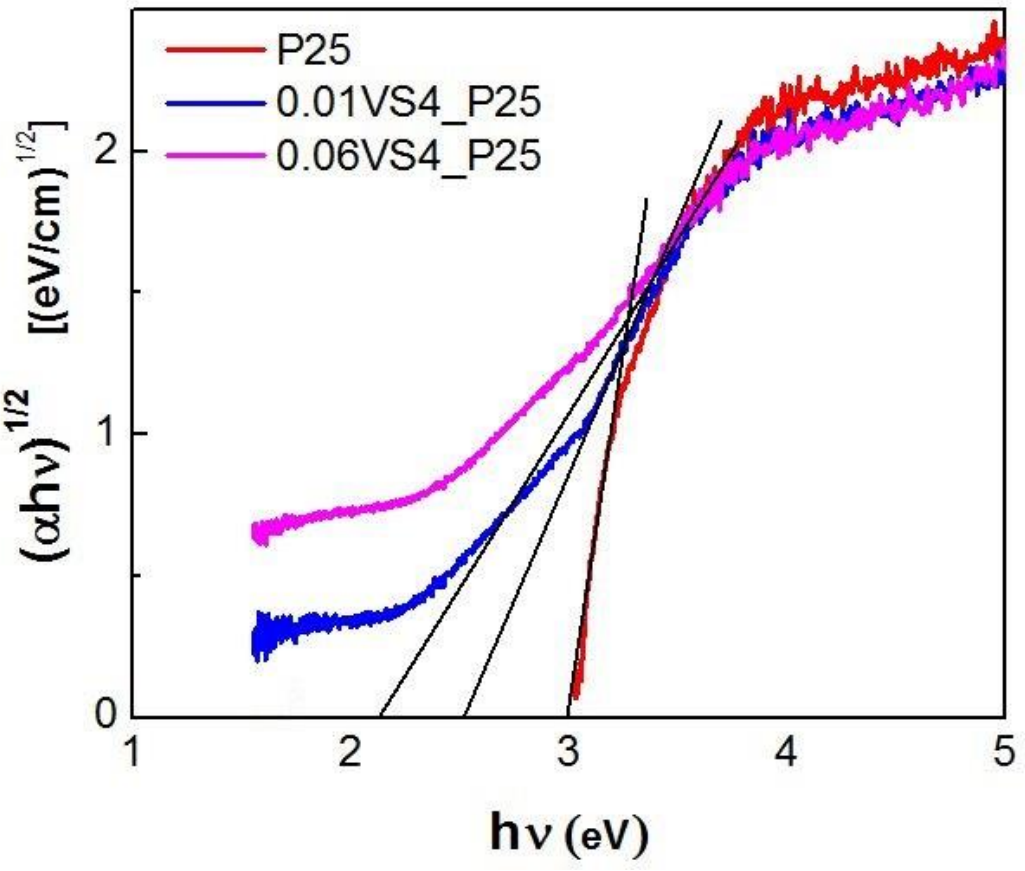

Figure 5-13 Tauc Plot of P25, 1 wt.% VS_4-on-P25, and 6 wt.% VS_4-on-P25; including the band gap estimations by extrapolating tangents to the abscissa

6. Conclusions and Future work

In summary, the VS_4 nanodiscs have been synthesized by apply a simple hydrothermal reaction, and the VS_4-on-P25 can be achieved via the same method. The VS_4-on-P25 heterostructures experience a significant improvement in photo-degradation of MB under UV irradiation. In this work, VS_4-on-P25 has been shown to be superior to P25 in photocatalytic performance by increase charge transfer rate along the coupled two semiconductors. Coupling VS_4 on P25 decreases the band gap of the pure TiO_2, lead to a wider light-absorption spectrum which greatly improves the photocatalytic activity at visible light range. Furthermore, this improved performance should also be ascribed to the adsorption ability of VS_4, which provides adsorption sites for MB, increases conductivity between the dye and photocatalyst, and suppresses charge carriers' recombination. The optimal VS_4 loading was found to be 6 wt.%. At this critical loading, the improved conductivity and adsorption of VS_4 balanced the best according to the experiment.

It is believed that this easy-synthesized novel heterostructured VS_4-on-P25 provides a new idea as a highly-active visible-light photocatalyst, not only in chemical deconstruction, but also in hydrogen production and even solar energy techniques.

Based on the existing results and a survey of present literatures, several recommendations can be proposed for future works. Firstly is to study VS_4 systematically, especially its physicochemical properties. Secondly, it is greatly needed to deeply investigate the

reaction mechanism of the synthesis of VS_4 to improve and perfect the synthesis of VS_4 with high crystallinity and purity. Thirdly, ground work of VS_4 on other different fields would also be very helpful for further understanding of this novel semiconductor material.

References

1. Fujishima A: **Electrochemical photolysis of water at a semiconductor electrode.** *Nature* 1972, **238:**37-38.

2. Chen C, Wang C, Yeh J: **Improvement of Odor Elimination and Anti-bacterial Activity of Polyester Fabrics Finished with Composite Emulsions of Nanometer Titanium Dioxide-silver Particles-water-borne Polyurethane.** *Text Res J* 2010, **80**(4)**:**291-300.

3. Sopyan I, Watanabe M, Murasawa S, Hashimoto K, Fujishima A: **An efficient TiO2 thin-film photocatalyst: photocatalytic properties in gas-phase acetaldehyde degradation.** *J Photochem Photobiol A* 1996, **98**(1-2)**:**79-86.

4. Zhao X, Zhao Q, Yu J, Liu B: **Development of multifunctional photoactive self-cleaning glasses.** *J Non Cryst Solids* 2008, **354**(12-13)**:**1424-1430.

5. Watanabe T, Nakajima A, Wang R, Minabe M, Koizumi S, Fujishima A, Hashimoto K: **Photocatalytic activity and photoinduced hydrophilicity of titanium dioxide coated glass.** *Thin Solid Films* 1999, **351**(1-2)**:**260-263.

6. Dal'Acqua N, Scheffer FR, Boniatti R, da Silva BVM, de Melo JV, da Silva Crespo J, Giovanela M, Pereira MB, Weibel DE, Machado G: **Photocatalytic Nanostructured Self-Assembled Poly(allylamine hydrochloride)/Poly(acrylic acid) Polyelectrolyte Films Containing Titanium Dioxide–Gold Nanoparticles for Hydrogen Generation.** *J Phys Chem C* 2013, **117**(44)**:**23235-23243.

7. Guo S, Han S, Mao H, Dong S, Wu C, Jia L, Chi B, Pu J, Li J: **Structurally controlled ZnO/TiO2 heterostructures as efficient photocatalysts for hydrogen generation from water without noble metals: The role of microporous amorphous/crystalline composite structure.** *J Power Sources* 2014, **245**(0)**:**979-985.

8. Rayalu SS, Jose D, Joshi MV, Mangrulkar PA, Shrestha K, Klabunde K: **Photocatalytic water splitting on Au/TiO2 nanocomposites synthesized through various routes: Enhancement in photocatalytic activity due to SPR effect.** *Applied Catalysis B: Environmental* 2013, **142–143**(0)**:**684-693.

9. Vorontsov AV, Besov AS, Parmon VN: **Fast purification of air from diethyl sulfide with nanosized TiO2 aerosol.** *Applied Catalysis B: Environmental* 2013, **129:**318-324.

10. Lv J, Zhu L: **Highly efficient indoor air purification using adsorption-enhanced-photocatalysis-based microporous TiO2 at short residence time.** *Environ Technol* 2013, **34**(11)**:**1447-1454.

11. Su C, Ran X, Hu J, Shao C: **Photocatalytic Process of Simultaneous Desulfurization and Denitrification of Flue Gas by TiO2–Polyacrylonitrile Nanofibers.** *Environ Sci Technol* 2013, **47**(20)**:**11562-11568.

12. Bai H, Liu L, Liu Z, Sun DD: **Hierarchical 3D dendritic TiO2 nanospheres building with ultralong 1D nanoribbon/wires for high performance concurrent photocatalytic membrane water purification.** *Water Res* 2013, **47**(12)**:**4126-4138.

13. Liu L, Bai H, Liu J, Sun DD: **Multifunctional graphene oxide-TiO2-Ag nanocomposites for high performance water disinfection and decontamination under solar irradiation.** *J Hazard Mater* 2013, **261**(6)**:**214-223.

14. Wei X, Cui H, Guo S, Zhao L, Li W: **Hybrid BiOBr–TiO2 nanocomposites with high visible light photocatalytic activity for water treatment.** *J Hazard Mater* 2013, **263, Part 2**(0)**:**650-658.

15. Renz C: **Photoreactions of oxides of titanium, cerium and earth acids.** *Helvetica chimica acta* 1921, (4)**:**961-968.

16. Tan ST, Umar AA, Balouch A, Yahaya M, Yap CC, Salleh MM, Oyama M: **ZnO nanocubes with (101) basal plane photocatalyst prepared via a low-frequency ultrasonic assisted hydrolysis process.** *Ultrasonics - Sonochemistry* 2014, **21**(2)**:**754-760.

17. Amano F, Ishinaga E, Yamakata A: **Effect of Particle Size on the Photocatalytic Activity of WO3 Particles for Water Oxidation.** *J Phys Chem C* 2013, **117**(44)**:**22584-22590.

18. Wang J, Fang T, Yan S, Li Z, Yu T, Zou Z: **Highly efficient visible light photocatalytic activity of Cr–La codoped SrTiO3 with surface alkalinization: An insight from DFT calculation.** *Computational Materials Science* 2013, **79**(19)**:**87-94.

19. Pradhan GK, Padhi DK, Parida KM: **Fabrication of a-Fe2O3 Nanorod/RGO Composite: A Novel Hybrid Photocatalyst for Phenol Degradation.** *ACS Appl Mater Interfaces* 2013, **5**(18)**:**9101-9110.

20. Chen J, Xin F, Qin S, Yin X: **Photocatalytically reducing CO2 to methyl formate in methanol over ZnS and Ni-doped ZnS photocatalysts.** *Chem Eng J* 2013, **230**(6)**:**506-512.

21. Yan S, Wang B, Shi Y, Yang F, Hu D, Xu X, Wu J: **Hydrothermal synthesis of CdS nanoparticle/functionalized graphene sheet nanocomposites for visible-light photocatalytic degradation of methyl orange.** *Appl Surf Sci* 2013, **285:**840-845.

22. Zhu H, Li Q: **Visible light-driven CdSe nanotube array photocatalyst.** *Nanoscale Res Lett* 2013, **8**(1)**:**1-6.

23. Torimoto T, Sakata T, Mori H, Yoneyama H: **Effect of Surface Charge of 4-Aminothiophenol-Modified PbS Microcrystal Photocatalysts on Photoinduced Charge Transfer.** *The Journal of Physical Chemistry* 1994, **98**(11)**:**3036-3043.

24. Amy L. Linsebigler , Guangquan. Lu , John T. Yates: **Photocatalysis on TiO2 Surfaces: Principles, Mechanisms, and Selected Results.** *Chemical reviews* 1995, **95**(3)**:**735–758.

25. Yang L, Liu Z: **Study on light intensity in the process of photocatalytic degradation of indoor gaseous formaldehyde for saving energy.** *Energy Conversion and Management* 2007, **48**(3)**:**882-889.

26. Tayade RJ, Kulkarni RG, Jasra RV: **Transition Metal Ion Impregnated Mesoporous TiO2 for Photocatalytic Degradation of Organic Contaminants in Water.** *Ind Eng Chem Res* 2006, **45**(15)**:**5231-5238.

27. Shamsipur M, Reza Rajabi H, Khani O: **Pure and Fe3+-doped ZnS quantum dots as novel and efficient nanophotocatalysts: Synthesis, characterization and use for decolorization of Victoria blue R.** *Materials Science in Semiconductor Processing* 2013, **16**(4)**:**1154-1161.

28. McManamon C, Delaney P, Morris MA: **Photocatalytic properties of metal and non-metal doped novel sub 10nm titanium dioxide nanoparticles on methyl orange.** *J Colloid Interface Sci* 2013, **411**(10)**:**169-172.

29. Zhang C, Jia Y, Jing Y, Yao Y, Ma J, Sun J: **Effect of non-metal elements (B, C, N, F, P, S) mono-doping as anions on electronic structure of SrTiO3.** *Computational Materials Science* 2013, **79**(8)**:**69-74.

30. Devi LG, Kavitha R: **A review on non metal ion doped titania for the photocatalytic degradation of organic pollutants under UV/solar light: Role of photogenerated charge carrier dynamics in enhancing the activity.** *Applied Catalysis B: Environmental* 2013, **140-141**(4)**:**559-587.

31. Kim SH, Jung C, Sahu N, Park D, Yun JY, Ha H, Park JY: **Catalytic activity of Au/TiO2 and Pt/TiO2 nanocatalysts prepared with arc plasma deposition under CO oxidation.** *Applied Catalysis A, General* 2013, **454:**53-58.

32. Kong L, Jiang Z, Lai HH-, Xiao T, Edwards PP: **Does noble metal modification improve the photocatalytic activity of BiOCl?** *Progress in Natural Science: Materials International* 2013, **23**(3)**:**286-293.

33. Iwahara N, Sato T, Tanaka K, Tanaka T: **Vibronically induced activation mechanism in photocatalysis of highly dispersed vanadium oxide supported on silica, V2O5/SiO2: Evidence in phosphorescence spectra.** *Chemical Physics Letters* 2013, **584**(11-12)**:**63-66.

34. Shih T, Lin C, Hsu I, Chen J, Sun Y: **Development of a Titanium Dioxide-Coated Microfluidic-Based Photocatalyst-Assisted Reduction Device to Couple High-Performance Liquid Chromatography with Inductively Coupled Plasma-Mass Spectrometry for Determination of Inorganic Selenium Species.** *Anal Chem* 2013, **85**(21)**:**10091-10098.

35. Castro CA, Centeno A, Giraldo SA: **Iron promotion of the TiO2 photosensitization process towards the photocatalytic oxidation of azo dyes under solar-simulated light irradiation.** *Materials Chemistry and Physics* 2011, **129**(3)**:**1176-1183.

36. Li Z, He L, Jing L, Lin J, Luan Y: **Facile Synthesis of Phosphate-Functionalized MWCNT-TiO2 Nanocomposites as Efficient Photocatalysts and Insights into the Roles of Nanostructured Carbon.** *ChemPlusChem* 2013, **78**(7)**:**670-676.

37. Chhowalla M, Shin HS, Eda G, Li LJ, Loh KP, Zhang H.: **The chemistry of two-dimensional layered transition metal dichalcogenide nanosheets.** *Nature chemistry* 2013, **5**(4)**:**263 -275.

38. Abu El-Oyoun M: **DSC studies on the transformation kinetics of two separated crystallization peaks of Si12.5Te87.5 chalcogenide glass: An application of the theoretical method developed and isoconversional method.** *Materials Chemistry and Physics* 2011, **131**(1-2)**:**495-506.

39. Evaristo M, Polcar T, Cavaleiro A: **Synthesis and properties of W–Se–C coatings deposited by PVD in reactive and non-reactive processes.** *Vacuum* 2009, **83**(10)**:**1262-1265.

40. Ganal P, Olberding W, Butz T, Ouvrard G: **Soft chemistry induced host metal coordination change from octahedral to trigonal prismatic in 1T-TaS2.** *Solid State Ionics* 1993, **59**(3-4)**:**313-319.

41. Ge W, Kawahara K, Tsuji M: **Large-scale synthesis of NbS2 nanosheets with controlled orientation on graphene by ambient pressure CVD.** *Nanoscale* 2013, **5**(13)**:**5773 -5778.

42. Jeong S, Yoo D, Jang J, Kim M, Cheon J: **Well-Defined Colloidal 2-D Layered Transition-Metal Chalcogenide Nanocrystals via Generalized Synthetic Protocols.** *J Am Chem Soc* 2012, **134**(44)**:**18233-18236.

43. Jing D, Guo L: **WS2 sensitized mesoporous TiO2 for efficient photocatalytic hydrogen production from water under visible light irradiation.** *Catalysis Communications* 2007, **8**(5)**:**795-799.

44. Li H, Ma L, Chen W, Wang J: **Synthesis of MoS2/C nanocomposites by hydrothermal route used as Li-ion intercalation electrode materials.** *Mater Lett* 2009, **63**(15)**:**1363-1365.

45. Linganiso EC, Mhlanga SD, Coville NJ, Mwakikunga BW: **Size-dependent and intra-band photoluminescence of NiS2 nano-alloys synthesized by microwave assisted hydrothermal technique.** *J Alloys Compounds* 2013, **552**(0)**:**345-350.

46. Parsapour F, Kelley DF, Williams RS: **Spectroscopy of Eu3+-Doped PtS2 Nanoclusters.** *The Journal of Physical Chemistry B* 1998, **102**(41)**:**7971-7977.

47. Peters ES, Carmalt CJ, Parkin IP: **Dual-source chemical vapour deposition of titanium sulfide thin films from tetrakisdimethylamidotitanium and sulfur precursors.** *Journal of Materials Chemistry* 2004, **14**(23)**:**3474-3477.

48. Qiu B, Zhao X, Xia D: **In situ synthesis of CoS2/RGO nanocomposites with enhanced electrode performance for lithium-ion batteries.** *J Alloys Compounds* 2013, **579**(0)**:**372-376.

49. Sepúlveda C, Escalona N, Garcá R, Laurenti D, Vrinat M: **Hydrodeoxygenation and hydrodesulfurization co-processing over ReS2 supported catalysts.** *Catalysis Today* 2012, **195**(1)**:**101-105.

50. Shimakawa M, Kawachi K, Nishikawa S, Hayashi K: **Structural Stability of the 1T Structure on Transition-Metal Dichalcogenides.** *Journal of Solid State Chemistry* 1997, **129**(2)**:**242-249.

51. Soulard C, Rocquefelte X, Petit P-, Evain M, Jobic S, Itié J-, Munsch P, Koo H-, Whangbo M-: **Experimental and Theoretical Investigation on the Relative Stability of the PdS2- and Pyrite-Type Structures of PdSe2.** *Inorg Chem* 2004, **43**(6)**:**1943-1949.

52. Wakatsuki Y, Yamazaki H, Cheng C: **The reaction of elemental sulfur with Rh(η5-C5H4Z)(PPh3)(2 (Z = H, CO2Me). Formation of RhS4, RhS5, RhS6, and (RhS2)2 catenated metallacycle complexes.** *Journal of Organometallic Chemistry* 1989, **372**(3)**:**437-445.

53. Weck PF, Kim E, Czerwinski KR: **Semiconducting layered technetium dichalcogenides: insights from first-principles.** *Dalton Trans* 2013, **42**(43)**:**15288-15295.

54. Zeng Z, Yin Z, Huang X, Li H, He Q, Lu G, Boey F, Zhang H: **Single-Layer Semiconducting Nanosheets: High-Yield Preparation and Device Fabrication.** *Angewandte Chemie International Edition* 2011, **50**(47)**:**11093-11097.

55. Manish Chhowalla, Hyeon Suk Shin, Goki Eda, Lain-Jong Li, Kian Ping Loh & Hua Zhang: **The chemistry of two-dimensional layered transition metal dichalcogenide nanosheets.** *Nature chemistry* 2013, **5**(4)**:**263 -275.

56. Jiang L, Zhu Y, Cui J: **Cetyltrimethylammonium bromide assisted self-assembly of NiTe2 nanoflakes: Nanoflake arrays and their photoluminescence properties.** *Journal of Solid State Chemistry* 2010, **183**(10)**:**2358-2364.

57. Zhang Y, Wu X: **Vanadium sulfide nanoribbons: Electronic and magnetic properties.** *Physics Letters A* 2013, **377**(43)**:**3154-3157.

58. Feng J, Sun X, Wu C, Peng L, Lin C, Hu S, Yang J, Xie Y: **Metallic Few-Layered VS2 Ultrathin Nanosheets: High Two-Dimensional Conductivity for In-Plane Supercapacitors.** *J Am Chem Soc* 2011, **133**(44)**:**17832-17838.

59. Feng J, Peng L, Wu C, Sun X, Hu S, Lin C, Dai J, Yang J, Xie Y: **Giant Moisture Responsiveness of VS2 Ultrathin Nanosheets for Novel Touchless Positioning Interface.** *ADVANCED MATERIALS* 2012, **24**(15)**:**1969-1974.

60. Fröschl T, Hörmann U, Kubiak P, Kucerová G, Pfanzelt M, Weiss CK, Behm RJ, Hüsing N, Kaiser U, Landfester K, Wohlfahrt-Mehrens M: **High surface area crystalline titanium dioxide: potential and limits in electrochemical energy storage and catalysis.** *Chem Soc Rev* 2012, **41**(15)**:**5313-5360.

61. Fujishima A, Zhang X, Tryk DA: **TiO2 photocatalysis and related surface phenomena.** *Surface Science Reports* 2008, **63**(12)**:**515-582.

62. Sclafani A, Herrmann JM: **Comparison of the Photoelectronic and Photocatalytic Activities of Various Anatase and Rutile Forms of Titania in Pure Liquid Organic Phases and in Aqueous Solutions.** *J Phys Chem* 1996, **100**(32)**:**13655-13661.

63. Hadjiivanov KI, Klissurski DG: **Surface chemistry of titania (anatase) and titania-supported catalysts.** *Chem Soc Rev* 1996, **25**(1)**:**61-69.

64. Dolata M, Kedzierzawski P, Augustynski J: **Comparative impedance spectroscopy study of rutile and anatase Tio2 film electrodes.** *Electrochim Acta* 1996, **41**(7–8)**:**1287-1293.

65. Zhang H, Banfield JF: **Understanding Polymorphic Phase Transformation Behavior during Growth of Nanocrystalline Aggregates: Insights from TiO2.** *The Journal of Physical Chemistry B* 2000, **104**(15)**:**3481-3487.

66. Shklover V, Nazeeruddin M-, Zakeeruddin SM, Barbé C, Kay A, Haibach T, Steurer W, Hermann R, Nissen H-, Grätzel M: **Structure of Nanocrystalline TiO2 Powders and Precursor to Their Highly Efficient Photosensitizer.** *Chemistry of Materials* 1997, **9**(2)**:**430-439.

67. Mamakhel A, Tyrsted C, Bøjesen ED, Hald P, Iversen BB: **Direct Formation of Crystalline Phase Pure Rutile TiO2 Nanostructures by a Facile Hydrothermal Method.** *Cryst Growth Des* 2013, **13**(11)**:**4730-4734.

68. - Chen JS, - Ng MF, - Wu HB, - Zhang L, - Lou XW(: - **Synthesis of phase-pure SnO2 nanosheets with different organized structures and their lithium storage properties.** - *CrystEngComm* (- 16)**:**- 5133.

69. Sabale S, Bandgar A, Wang H, Gurav K, Kim J, Pawar S: **Direct synthesis and characterization of high temperature stable anatase TiO2 nanospheres from peroxo-titanium complex.** *Met Mater Int* 2013, **19**(3)**:**483-488.

70. Diebold U: **The surface science of titanium dioxide.** *Surface Science Reports* 2003, **48**(5-8)**:**53-229.

71. Ramamoorthy M, Vanderbilt D, King-Smith RD: **First-principles calculations of the energetics of stoichiometric TiO2 surfaces.** *Physics Reviews* 1994, **49**(23)**:**721-727.

72. Hengerer R, Bolliger B, Erbudak M, Grätzel M: **Structure and stability of the anatase TiO2 (101) and (001) surfaces.** *Surf Sci* 2000, **460**(1–3)**:**162-169.

73. Liang Y, Gan S, Chambers S: **Surface structure of anatase TiO2(001): Reconstruction, atomic steps, and domains.** *Physical review. B* 2001, **63**(23)**:**235402:1-7.

74. Ruzycki N, Herman GS, Boatner LA, Diebold U: **Scanning tunneling microscopy study of the anatase (1 0 0) surface.** *Surf Sci* 2003, **529**(1–2)**:**L239-L244.

75. - Goodeve CF, - Kitchener JA: - **Photosensitisation by titanium dioxide.** - *Trans Faraday Soc* (- 0)**:**- 570.

76. A. E. Jacobsen: **Titanium Dioxide Pigments: Correlation between Photochemical Reactivity and Chalking..** *Industrial & engineering chemistry* 1949, **41**(3)**:**523-526.

77. - McLintock IS, - Ritchie M: - **Reactions on titanium dioxide; photo-adsorption and oxidation of ethylene and propylene.** - *Trans Faraday Soc* (- 0)**:**- 1007.

78. FUJISHIMA A, KOHAYAKAWA K, HONDA K: **Hydrogen Production under Sunlight with an Electrochemical Photocell.** *Journal of the Electrochemical Society* 1975, **122**(11)**:**1487 -1489.

79. M.R. Hoffmann, S.T. Martin, W. Choi, D.W. Bahnemann: **Environmental Applications of Semiconductor Photocatalysis.** *Chemical reviews* 1994, **95**(1)**:**69–96.

80. - Tamaki Y, - Furube A, - Murai M, - Hara K, - Katoh R, - Tachiya M: **- Dynamics of efficient electron-hole separation in TiO2 nanoparticles revealed by femtosecond transient absorption spectroscopy under the weak-excitation condition.** - *Phys Chem Chem Phys* (- 12)**:**- 1453.

81. A.M. Peiro, C. Colombo, G. Doyle, J. Nelson, A. Mills, J.R. Durrant,: **Photochemical reduction of oxygen adsorbed to nanocrystalline TiO(2) films: a transient absorption and oxygen scavenging study of different TiO(2) preparations..** *J Phys Chem B* 2006, **110**(46)**:**23255–23263.

82. Yoshihara T, Katoh R, Furube A, Tamaki Y, Murai M, Hara K, Murata S, Arakawa H, Tachiya M: **Identification of Reactive Species in Photoexcited Nanocrystalline TiO2 Films by Wide-Wavelength-Range (400-2500 nm) Transient Absorption Spectroscopy.** *The Journal of Physical Chemistry B* 2004, **108**(12)**:**3817-3823.

83. Horváth IT: *Encyclopedia of catalysis:* Hoboken, NJ, USA: John Wiley and Sons, Inc; 2003.

84. Tamaki Y, Furube A, Murai M, Hara K, Katoh R, Tachiya M: **Direct Observation of Reactive Trapped Holes in TiO2 Undergoing Photocatalytic Oxidation of Adsorbed Alcohols: Evaluation of the Reaction Rates and Yields.** *J Am Chem Soc* 2006, **128**(2)**:**416-417.

85. Yamakata A, Ishibashi T, Onishi H: **Water- and Oxygen-Induced Decay Kinetics of Photogenerated Electrons in TiO2 and Pt/TiO2: A Time-Resolved Infrared Absorption Study.** *The Journal of Physical Chemistry B* 2001, **105**(30)**:**7258-7262.

86. Murai M, Tamaki Y, Furube A, Hara K, Katoh R: **Reaction of holes in nanocrystalline TiO2 films evaluated by highly sensitive transient absorption spectroscopy.** *Catalysis Today* 2007, **120**(2)**:**214-219.

87. Iwata K, Takaya T, Hamaguchi H, Yamakata A, Ishibashi T, Onishi H, Kuroda H: **Carrier Dynamics in TiO2 and Pt/TiO2 Powders Observed by Femtosecond Time-Resolved Near-Infrared Spectroscopy at a Spectral Region of 0.9-1.5 μm with the Direct Absorption Method.** *The Journal of Physical Chemistry B* 2004, **108**(52)**:**20233-20239.

88. Gaya UI, Abdullah AH: **Heterogeneous photocatalytic degradation of organic contaminants over titanium dioxide: A review of fundamentals, progress and problems.** *Journal of Photochemistry & Photobiology, C: Photochemistry Reviews* 2008, **9**(1)**:**1-12.

89. Spacek W, Bauer R, Heisler G: **Heterogeneous and homogeneous wastewater treatment - comparison between photodegradation with TiO2 and the photo-Fenton reaction.** *Chemosphere* 1995, **30**(3)**:**477-484.

90. Hofstadler K, Bauer R, Novalic S, Heisler G: **New Reactor Design for Photocatalytic Wastewater Treatment with TiO2 Immobilized on Fused-Silica Glass Fibers: Photomineralization of 4-Chlorophenol.** *Environ Sci Technol* 1994, **28**(4)**:**670-674.

91. Pedroza AM, Mosqueda R, Alonso-Vante N, Rodriguez-Vazquez R: **Sequential treatment via Trametes versicolor and UV/TiO2/RuxSey to reduce contaminants in waste water resulting from the bleaching process during paper production.** *Chemosphere* 2007, **67**(4)**:**793-801.

92. Liu H, Dong X, Li G, Su X, Zhu Z: **Synthesis of C, Ag co-modified TiO2 photocatalyst and its application in waste water purification.** *Applied Surface Science* 2013, **271:**276-283.

93. Dey GR, Singh BN, Kumar SD, Das TN: **Dielectric Barrier Discharge Initiated Gas-Phase Decomposition of CO2 to CO and C6–C9 Alkanes to C1–C3 Hydrocarbons on Glass, Molecular Sieve 10X and TiO2/ZnO Surfaces.** *Plasma Chem Plasma Process* 2007, **27**(6)**:**669-678.

94. Burch R, Bond GC, Rajaram RR: **Hydrogenolysis of alkanes. Part 3.—Hydrogenolysis of n-hexane and methylcyclopentane over variously treated Ru/TiO2 catalysts.** *Journal of the Chemical Society, Faraday Transactions 1: Physical Chemistry in Condensed Phases* 1986, **82**(6)**:**1985-1998.

95. Sabin F, Türk T, Vogler A: **Photo-oxidation of organic compound in the presence of titanium dioxide: determination of the efficiency.** *J Photochem Photobiol A* 1992, **63**(1)**:**99-106.

96. Obare SO, Ito T, Meyer GJ: **Controlling Reduction Potentials of Semiconductor-Supported Molecular Catalysts for Environmental Remediation of Organohalide Pollutants.** *Environ Sci Technol* 2005, **39**(16)**:**6266-6272.

97. Franking R, Kim H, Chambers SA, Mangham AN, Hamers RJ: **Photochemical Grafting of Organic Alkenes to Single-Crystal TiO2 Surfaces: A Mechanistic Study.** *Langmuir* 2012, **28**(33)**:**12085-12093.

98. Kodama S, Yagi S: **Photocatalytic hydrogenation, decomposition and isomerization reactions of alkenes over TiO2-adsorbed water.** *Journal of the Chemical Society, Faraday Transactions* 1992, **88**(12)**:**1685-1690.

99. Wang N, Zhu L, Huang Y, She Y, Yu Y, Tang H: **Drastically enhanced visible-light photocatalytic degradation of colorless aromatic pollutants over TiO2 via a charge-transfer-complex path: A correlation between chemical structure and degradation rate of the pollutants.** *Journal of Catalysis* 2009, **266**(2)**:**199-206.

100. Zhang Y, Tang Z, Fu X, Xu Y: **TiO2-Graphene Nanocomposites for Gas-Phase Photocatalytic Degradation of Volatile Aromatic Pollutant: Is TiO2-Graphene Truly Different from Other TiO2-Carbon Composite Materials?** *ACS Nano* 2010, **4**(12)**:**7303-7314.

101. Múcka V, Cuba V, Silber R, Pospíšil M: **Reaction orders of radiation-induced dechlorinations of some aliphatic chlorinated hydrocarbons in aqueous solutions.** *Radiat Phys Chem* 2009, **78**(4)**:**261-266.

102. Augugliaro V, Kisch H, Loddo V, López-Muñoz MJ, Márquez-Álvarez C, Palmisano G, Palmisano L, Parrino F, Yurdakal S: **Photocatalytic oxidation of aromatic alcohols to aldehydes in aqueous suspension of home-prepared titanium dioxide.** *Applied Catalysis A, General* 2008, **349**(1-2)**:**182-188.

103. Lambropoulou DA, Konstantinou IK, Albanis TA, Fernández-Alba AR: **Photocatalytic degradation of the fungicide Fenhexamid in aqueous TiO2 suspensions: Identification of intermediates products and reaction pathways.** *Chemosphere* 2011, **83**(3)**:**367-378.

104. Anonymous - **Spectroscopic monitoring of photocatalytic degradation of the insecticide acetamiprid and its degradation product 6-chloronicotinic acid on TiO2 catalyst.** - *Journal of Environmental Science and Health, Part A* (- 12)**:**- 1919.

105. Tang Y, Zhang G, Liu C, Luo S, Xu X, Chen L, Wang B: **Magnetic TiO2-graphene composite as a high-performance and recyclable platform for efficient photocatalytic removal of herbicides from water.** *Journal of Hazardous Materials* 2013, **252-253**(3)**:**115-122.

106. Seck EI, Doña-Rodríguez JM, Fernández-Rodríguez C, Portillo-Carrizo D, Hernández-Rodríguez MJ, González-Díaz OM, Pérez-Peña J: **Solar photocatalytic removal of herbicides from real water by using sol–gel synthesized nanocrystalline TiO2: Operational parameters optimization and toxicity studies.** *Solar Energy* 2013, **87:**150-157.

107. Abramovic BF, Despotovic VN, Šojic DV, Orcic DZ, Csanádi JJ, Cetojevic-Simin DD: **Photocatalytic degradation of the herbicide clomazone in natural water using TiO2: Kinetics, mechanism, and toxicity of degradation products.** *Chemosphere* 2013, **93**(1)**:**166-171.

108. Zhou Q, Huang Y, Xiao J, Xie G: **Micro-solid phase equilibrium extraction with highly ordered TiO2 nanotube arrays: a new approach for the enrichment and measurement of organochlorine pesticides at trace level in environmental water samples.** *Anal Bioanal Chem* 2011, **400**(1)**:**205-212.

109. Lhomme L, Brosillon S, Wolbert D: **Photocatalytic degradation of pesticides in pure water and a commercial agricultural solution on TiO2 coated media.** *Chemosphere* 2008, **70**(3)**:**381-386.

110. Wang J, Zhou S, Wang J, Li S, Gao J, Wang B, Fan P: **Improvement of sonocatalytic activity of TiO2 by using Yb, N and F-doped Er3+:Y3Al5O12 for degradation of organic dyes.** *Ultrasonics - Sonochemistry* 2014, **21**(1)**:**84-92.

111. Dianat S, Tangestaninejad S, Mirkhani V, Moghadam M, Mohammadpoor-Baltork I: **Preparation, characterization and photocatalytic properties of InVO4 nanopowder and InVO4–TiO2 nanocomposite toward degradation of azo dyes and formaldehyde under visible light and ultrasonic irradiation.** *J IRAN CHEM SOC* 2013, **10**(3)**:**535-544.

112. Abd El-Rehim HA, Hegazy EA, Diaa DA: **Photo-catalytic degradation of Metanil Yellow dye using TiO2 immobilized into polyvinyl alcohol/acrylic acid microgels prepared by ionizing radiation.** *React Funct Polym* 2012, **72**(11)**:**823-831.

113. Adamcíková L, Pavlíková K, Ševcík P: **The methylene blue-D-glucose-O2 system. Oxidation of D-glucose by methylene blue in the presence and the absence of oxygen.** *Int J Chem Kinet* 1999, **31**(6)**:**463-468.

114. Tang D, Santschi PH: **Sensitive determination of dissolved sulfide in estuarine water by solid-phase extraction and high-performance liquid chromatography of methylene blue.** *Journal of Chromatography A* 2000, **883**(1-2)**:**305-309.

115. Watcharenwong A, Chanmanee W, de Tacconi NR, Chenthamarakshan CR, Kajitvichyanukul P, Rajeshwar K: **Anodic growth of nanoporous WO3 films: Morphology, photoelectrochemical response and photocatalytic activity for methylene blue and hexavalent chrome conversion.** *J Electroanal Chem* 2008, **612**(1)**:**112-120.

116. Skúladóttir G, Shi-Hua D, Brodie A, Reed D, Wander R: **Effects of dietary oils and methyl ethyl ketone peroxide onin vivo lipid peroxidation and antioxidants in rat heart and liver.** *Lipids* 1994, **29**(5)**:**351-357.

117. Du M, Yang T, Zhang Y, Jiao K: **Sensitively Electrochemical Sensing for Sequence-Specific Detection of Phosphinothricin Acetyltransferase Gene: Layer-by-Layer Films of Poly-L-Lysine and Au-Carbon Nanotube Hybrid.** *Electroanalysis* 2009, **21**(23)**:**2521-2526.

118. Zhang D, Peng Y, Qi H, Gao Q, Zhang C: **Label-free electrochemical DNA biosensor array for simultaneous detection of the HIV-1 and HIV-2 oligonucleotides incorporating different hairpin-DNA probes and redox indicator.** *Biosensors and Bioelectronics* 2010, **25**(5)**:**1088-1094.

119. Lachheb H, Puzenat E, Houas A, Ksibi M, Elaloui E, Guillard C, Herrmann J: **Photocatalytic degradation of various types of dyes (Alizarin S, Crocein Orange G, Methyl Red, Congo Red, Methylene Blue) in water by UV-irradiated titania.** *Applied Catalysis B: Environmental* 2002, **39**(1)**:**75-90.

120. ZhangPermanent address: Department of Applied Chemistry, College of Chemical Engineering and Technology, Tianjin University, Tianjin 300072,PR China., Tianyong, Oyama T, Aoshima A, Hidaka H, Zhao J, Serpone N: **Photooxidative N-demethylation of methylene blue in aqueous TiO2 dispersions under UV irradiation.** *J Photochem Photobiol A* 2001, **140**(2)**:**163-172.

121. Li XZ, Li FB, Yang CL, Ge WK: **Photocatalytic activity of WOx-TiO2 under visible light irradiation.** *J Photochem Photobiol A* 2001, **141**(2-3)**:**209-217.

122. Zhang Y, Ma L, Li J, Yu Y: **In Situ Fenton Reagent Generated from TiO2/Cu2O Composite Film: a New Way to Utilize TiO2 under Visible Light Irradiation.** *Environ Sci Technol* 2007, **41**(17)**:**6264-6269.

123. Ohno T, Akiyoshi M, Umebayashi T, Asai K, Mitsui T, Matsumura M: **Preparation of S-doped TiO2 photocatalysts and their photocatalytic activities under visible light.** *Applied Catalysis A: General* 2004, **265**(1)**:**115-121.

124. Pelizzetti E, Minero C: **Mechanism of the photo-oxidative degradation of organic pollutants over TiO2 particles.** *Electrochim Acta* 1993, **38**(1)**:**47-55.

125. Guo Z, Ma R, Li G: **Degradation of phenol by nanomaterial TiO2 in wastewater.** *Chem Eng J* 2006, **119**(1)**:**55-59.

126. Yu J, Chi R, Guo J, Zhang Y, Xu Z, Xiao C: **Desorption and photodegradation of methylene blue from modified sugarcane bagasse surface by acid TiO2 hydrosol.** *Applied Surface Science* 2012, **258**(8)**:**4085-4090.

127. Houas A, Lachheb H, Ksibi M, Elaloui E, Guillard C, Herrmann J: **Photocatalytic degradation pathway of methylene blue in water.** *Applied Catalysis B: Environmental* 2001, **31**(2)**:**145-157.

128. Fetterolf ML, Patel HV, Jennings JM: **Adsorption of Methylene Blue and Acid Blue 40 on Titania from Aqueous Solution.** *Journal of Chemical & Engineering Data* 2003, **48**(4)**:**831-835.

129. Xiong L, Yang Y, Mai J, Sun W, Zhang C, Wei D, Chen Q, Ni J: **Adsorption behavior of methylene blue onto titanate nanotubes.** *Chem Eng J* 2010, **156**(2)**:**313-320.

130. Messina PV, Schulz PC: **Adsorption of reactive dyes on titania-silica mesoporous materials.** *J Colloid Interface Sci* 2006, **299**(1)**:**305-320.

131. Zhang T, Oyama Tk, Horikoshi S, Hidaka H, Zhao J, Serpone N: **Photocatalyzed N-demethylation and degradation of methylene blue in titania dispersions exposed to concentrated sunlight.** *Solar Energy Mater Solar Cells* 2002, **73**(3)**:**287-303.

132. Muruganandham M, Swaminathan M: **Solar photocatalytic degradation of a reactive azo dye in TiO2-suspension.** *Solar Energy Mater Solar Cells* 2004, **81**(4)**:**439-457.

133. Sivalingam G, Nagaveni K, Hegde MS, Madras G: **Photocatalytic degradation of various dyes by combustion synthesized nano anatase TiO2.** *Applied Catalysis B: Environmental* 2003, **45**(1)**:**23-38.

134. Sauer T, Cesconeto Neto G, José HJ, Moreira RFPM: **Kinetics of photocatalytic degradation of reactive dyes in a TiO2 slurry reactor.** *J Photochem Photobiol A* 2002, **149**(1-3)**:**147-154.

135. Chakrabarti S, Dutta BK: **Photocatalytic degradation of model textile dyes in wastewater using ZnO as semiconductor catalyst.** *J Hazard Mater* 2004, **112**(3)**:**269-278.

136. Demeestere K, Visscher AD, Dewulf J, Leeuwen MV, Langenhove HV: **A new kinetic model for titanium dioxide mediated heterogeneous photocatalytic degradation of trichloroethylene in gas-phase.** *Applied Catalysis B: Environmental* 2004, **54**(4)**:**261-274.

137. Brezová V, Blažková A, Karpinský Ľ, Grošková J, Havlínová B, Jorík V, Čeppan M: **Phenol decomposition using Mn+/TiO2 photocatalysts supported by the sol-gel technique on glass fibres.** *J Photochem Photobiol A* 1997, **109**(2)**:**177-183.

138. Chen J, Yao M, Wang X: **Investigation of transition metal ion doping behaviors on TiO2 nanoparticles.** *J Nanopart Res* 2008, **10**(1)**:**163-171.

139. Dhananjeyan MR, Kandavelu V, Renganathan R: **An investigation of the effects of Cu2+ and heat treatment on TiO2 photooxidation of certain pyrimidines.** *Journal of Molecular Catalysis A: Chemical* 2000, **158**(2)**:**577-582.

140. Dvoranová D, Brezová V, Mazúr M, Malati MA: **Investigations of metal-doped titanium dioxide photocatalysts.** *Applied Catalysis B, Environmental* 2002, **37**(2)**:**91-105.

141. Frindell KL, Bartl MH, Robinson MR, Bazan GC, Popitsch A, Stucky GD: **Visible and near-IR luminescence via energy transfer in rare earth doped mesoporous titania thin films with nanocrystalline walls.** *Journal of Solid State Chemistry* 2003, **172**(1)**:**81-88.

142. Kemp TJ, McIntyre RA: **Transition metal-doped titanium(IV) dioxide: Characterisation and influence on photodegradation of poly(vinyl chloride).** *Polym Degrad Stab* 2006, **91**(1)**:**165-194.

143. Kudo A, Niishiro R, Iwase A, Kato H: **Effects of doping of metal cations on morphology, activity, and visible light response of photocatalysts.** *Chem Phys* 2007, **339**(1-3)**:**104-110.

144. Lahav M, Heleg-Shabtai V, Wasserman J, Katz E, Willner I, Dürr H, Hu Y, Bossmann SH: **Photoelectrochemistry with Integrated Photosensitizer-Electron Acceptor and Au-Nanoparticle Arrays.** *J Am Chem Soc* 2000, **122**(46)**:**11480-11487.

145. Long RQ, Yang RT: **The promoting role of rare earth oxides on Fe-exchanged TiO2-pillared clay for selective catalytic reduction of nitric oxide by ammonia.** *Applied Catalysis B: Environmental* 2000, **27**(2)**:**87-95.

146. López T, Hernandez-Ventura J, Gómez R, Tzompantzi F, Sánchez E, Bokhimi X, García A: **Photodecomposition of 2,4-dinitroaniline on Li/TiO2 and Rb/TiO2 nanocrystallite sol–gel derived catalysts.** *Journal of Molecular Catalysis A: Chemical* 2001, **167**(1–2)**:**101-107.

147. Mohamed RM, Mkhalid IA: **The effect of rare earth dopants on the structure, surface texture and photocatalytic properties of TiO2–SiO2 prepared by sol–gel method.** *J Alloys Compounds* 2010, **501**(1)**:**143-147.

148. Morawski AW, Grzechulska J, Kalucki K: **A new method for preparation of potassium-pillared layered titanate applied in photocatalysis.** *Journal of Physics and Chemistry of Solids* 1996, **57**(6-8)**:**1011-1017.

149. Nguyen-Phan T, Song MB, Kim EJ, Shin EW: **The role of rare earth metals in lanthanide-incorporated mesoporous titania.** *Microporous and Mesoporous Materials* 2009, **119**(1-3)**:**290-298.

150. Parida KM, Sahu N: **Visible light induced photocatalytic activity of rare earth titania nanocomposites.** *Journal of Molecular Catalysis.A, Chemical* 2008, **287**(1-2)**:**151-158.

151. Rauf MA, Meetani MA, Hisaindee S: **An overview on the photocatalytic degradation of azo dyes in the presence of TiO2 doped with selective transition metals.** *Desalination* 2011, **276**(1-3)**:**13-27.

152. Tang F, Xu B, Shi H, Qiu J, Fan Y: **The poisoning effect of Na+ and Ca2+ ions doped on the V2O5/TiO2 catalysts for selective catalytic reduction of NO by NH3.** *Applied Catalysis B, Environmental* 2010, **94**(1-2)**:**71-76.

153. Venkatachalam N, Palanichamy M, Arabindoo B, Murugesan V: **Alkaline earth metal doped nanoporous TiO2 for enhanced photocatalytic mineralisation of bisphenol-A.** *Catalysis Communications* 2007, **8**(7)**:**1088-1093.

154. Venkatachalam N, Palanichamy M, Murugesan V: **Sol-gel preparation and characterization of alkaline earth metal doped nano TiO2: Efficient photocatalytic degradation of 4-chlorophenol.** *Journal of Molecular Catalysis.A, Chemical* 2007, **273**(1-2)**:**177-185.

155. Wang Y, Hao Y, Cheng H, Ma J, Xu B, Li W, Cai S: **The photoelectrochemistry of transition metal-ion-doped TiO2 nanocrystalline electrodes and higher solar cell conversion efficiency based on Zn2+-doped TiO2 electrode.** *J Mater Sci* 1999, **34**(12)**:**2773-2779.

156. Xu A, Gao Y, Liu H: **The Preparation, Characterization, and their Photocatalytic Activities of Rare-Earth-Doped TiO2 Nanoparticles.** *Journal of Catalysis* 2002, **207**(2)**:**151-157.

157. Zhu J, Chen F, Zhang J, Chen H, Anpo M: **Fe^3^+-TiO2 photocatalysts prepared by combining sol-gel method with hydrothermal treatment and their characterization.** *Journal of Photochemistry & Photobiology, A: Chemistry* 2006, **180**(1-2)**:**196-204.

158. Zhu J, Deng Z, Chen F, Zhang J, Chen H, Anpo M, Huang J, Zhang L: **Hydrothermal doping method for preparation of Cr^3^+-TiO2 photocatalysts with concentration gradient distribution of Cr^3^+.** *Applied Catalysis B, Environmental* 2006, **62**(3-4)**:**329-335.

159. Zhu J, Zheng W, He B, Zhang J, Anpo M: **Characterization of Fe–TiO2 photocatalysts synthesized by hydrothermal method and their photocatalytic reactivity for photodegradation of XRG dye diluted in water.** *Journal of Molecular Catalysis A: Chemical* 2004, **216**(1)**:**35-43.

160. Fernández A, Lassaletta G, Jiménez VM, Justo A, González-Elipe AR, Herrmann J-, Tahiri H, Ait-Ichou Y: **Preparation and characterization of TiO2 photocatalysts supported on various rigid supports (glass, quartz and stainless steel). Comparative studies of photocatalytic activity in water purification.** *Applied Catalysis B: Environmental* 1995, **7**(1–2)**:**49-63.

161. PAZ Y, LUO Z, RABENBERG L, HELLER A: **PHOTOOXIDATIVE SELF-CLEANING TRANSPARENT TITANIUM-DIOXIDE FILMS ON GLASS.** *Journal of materials research* 1995, **10**(11)**:**2842 -2848.

162. Anpo M, Takeuchi M: **The design and development of highly reactive titanium oxide photocatalysts operating under visible light irradiation.** *Journal of Catalysis* 2003, **216**(1–2)**:**505-516.

163. Sun L, Li J, Wang CL, Li SF, Chen HB, Lin CJ: **An electrochemical strategy of doping Fe3+ into TiO2 nanotube array films for enhancement in photocatalytic activity.** *Solar Energy Mater Solar Cells* 2009, **93**(10)**:**1875-1880.

164. Zhang Z, Wang C, Zakaria R, Ying JY: **Role of Particle Size in Nanocrystalline TiO2-Based Photocatalysts.** *The Journal of Physical Chemistry B* 1998, **102**(52)**:**10871-10878.

165. CHOI W, TERMIN A, HOFFMANN M: **EFFECTS OF METAL-ION DOPANTS ON THE PHOTOCATALYTIC REACTIVITY OF QUANTUM-SIZED TIO2 PARTICLES.** *ANGEWANDTE CHEMIE-INTERNATIONAL EDITION IN ENGLISH* 1994, **33**(10)**:**1091-1092.

166. CHOI W, TERMIN A, HOFFMANN M: **THE ROLE OF METAL-ION DOPANTS IN QUANTUM-SIZED TIO2 - CORRELATION BETWEEN PHOTOREACTIVITY AND CHARGE-CARRIER RECOMBINATION DYNAMICS.** *Journal of physical chemistry* 1994, **98**(51)**:**13669-13679.

167. Fuerte A, Hernández-Alonso MD, Maira AJ, Martínez-Arias A, Fernández-García M, Conesa JC, Soria J: **Visible light-activated nanosized doped-TiO2 photocatalysts.** *Chemical Communications* 2001, **2001**(24)**:**2718-2719.

168. Tian B, Li C, Gu F, Jiang H, Hu Y, Zhang J: **Flame sprayed V-doped TiO2 nanoparticles with enhanced photocatalytic activity under visible light irradiation.** *Chem Eng J* 2009, **151**(1–3)**:**220-227.

169. Ranjit KT, Willner I, Bossmann SH, Braun AM: **Lanthanide Oxide Doped Titanium Dioxide Photocatalysts: Effective Photocatalysts for the Enhanced Degradation of Salicylic Acid and t-Cinnamic Acid.** *Journal of Catalysis* 2001, **204**(2)**:**305-313.

170. Liu Y, Chen X, Li J, Burda C: **Photocatalytic degradation of azo dyes by nitrogen-doped TiO2 nanocatalysts.** *Chemosphere* 2005, **61**(1)**:**11-18.

171. Xiao J, Peng T, Li R, Peng Z, Yan C: **Preparation, phase transformation and photocatalytic activities of cerium-doped mesoporous titania nanoparticles.** *Journal of Solid State Chemistry* 2006, **179**(4)**:**1161-1170.

172. Chen X, Lou Y-, Samia A , Burda C, Gole J : **Formation of Oxynitride as the Photocatalytic Enhancing Site in Nitrogen-Doped Titania Nanocatalysts: Comparison to a Commercial Nanopowder.** *Adv Funct Mater* 2005, **15**(1)**:**41-49.

173. Cong Y, Zhang J, Chen F, Anpo M: **Synthesis and Characterization of Nitrogen-Doped TiO2 Nanophotocatalyst with High Visible Light Activity.** *Journal of Physical Chemistry C* 2007, **111**(19)**:**6976-6982.

174. Ihara T, Miyoshi M, Iriyama Y, Matsumoto O, Sugihara S: **Visible-light-active titanium oxide photocatalyst realized by an oxygen-deficient structure and by nitrogen doping.** *Applied Catalysis B: Environmental* 2003, **42**(4)**:**403-409.

175. Lindgren T, Mwabora JM, Avendaño E, Jonsson J, Hoel A, Granqvist C, Lindquist S: **Photoelectrochemical and Optical Properties of Nitrogen Doped Titanium Dioxide Films Prepared by Reactive DC Magnetron Sputtering.** *The Journal of Physical Chemistry B* 2003, **107**(24)**:**5709-5716.

176. Nosaka Y, Matsushita M, Nishino J, Nosaka AY: **Nitrogen-doped titanium dioxide photocatalysts for visible response prepared by using organic compounds.** *Science and Technology of Advanced Materials* 2005, **6**(2)**:**143-148.

177. Sathish M, Viswanathan B, Viswanath RP, Gopinath CS: **Synthesis, Characterization, Electronic Structure, and Photocatalytic Activity of Nitrogen-Doped TiO2 Nanocatalyst.** *Chemistry of Materials* 2005, **17**(25)**:**6349-6353.

178. Zhang G, Zhang YC, Nadagouda M, Han C, O'Shea K, El-Sheikh SM, Ismail AA, Dionysiou DD: **Visible light-sensitized S, N and C co-doped polymorphic TiO2 for photocatalytic destruction of microcystin-LR.** *Applied Catalysis B: Environmental* 2014, **144**(5)**:**614-621.

179. Park Y, Kim W, Park H, Tachikawa T, Majima T, Choi W: **Carbon-doped TiO2 photocatalyst synthesized without using an external carbon precursor and the visible light activity.** *Applied Catalysis B, Environmental* 2009, **91**(1-2)**:**355-361.

180. Ren W, Ai Z, Jia F, Zhang L, Fan X, Zou Z: **Low temperature preparation and visible light photocatalytic activity of mesoporous carbon-doped crystalline TiO2.** *Applied Catalysis B, Environmental* 2007, **69**(3-4)**:**138-144.

181. Xu Y, Zhuang Y, Fu X: **New Insight for Enhanced Photocatalytic Activity of TiO2 by Doping Carbon Nanotubes: A Case Study on Degradation of Benzene and Methyl Orange.** *J Phys Chem C* 2010, **114**(6)**:**2669-2676.

182. Park JH, Kim S, Bard AJ: **Novel Carbon-Doped TiO2 Nanotube Arrays with High Aspect Ratios for Efficient Solar Water Splitting.** *Nano Letters* 2006, **6**(1)**:**24-28.

183. Yu JC, Ho W, Yu J, Yip H, Wong PK, Zhao J: **Efficient Visible-Light-Induced Photocatalytic Disinfection on Sulfur-Doped Nanocrystalline Titania.** *Environ Sci Technol* 2005, **39**(4)**:**1175-1179.

184. Tian H, Ma J, Li K, Li J: **Hydrothermal synthesis of S-doped TiO2 nanoparticles and their photocatalytic ability for degradation of methyl orange.** *Ceram Int* 2009, **35**(3)**:**1289-1292.

185. Liu S, Chen X: **A visible light response TiO2 photocatalyst realized by cationic S-doping and its application for phenol degradation.** *J Hazard Mater* 2008, **152**(1)**:**48-55.

186. Rengifo-Herrera JA, Pulgarin C: **Photocatalytic activity of N, S co-doped and N-doped commercial anatase TiO2 powders towards phenol oxidation and E. coli inactivation under simulated solar light irradiation.** *Solar Energy* 2010, **84**(1)**:**37-43.

187. Sun H, Bai Y, Cheng Y, Jin W, Xu N: **Preparation and Characterization of Visible-Light-Driven Carbon-Sulfur-Codoped TiO2 Photocatalysts.** *Ind Eng Chem Res* 2006, **45**(14)**:**4971-4976.

188. Chen D, Yang D, Wang Q, Jiang Z: **Effects of Boron Doping on Photocatalytic Activity and Microstructure of Titanium Dioxide Nanoparticles.** *Ind Eng Chem Res* 2006, **45**(12)**:**4110-4116.

189. Huang Y, Ho W, Ai Z, Song X, Zhang L, Lee S: **Aerosol-assisted flow synthesis of B-doped, Ni-doped and B–Ni-codoped TiO2 solid and hollow microspheres for photocatalytic removal of NO.** *Applied Catalysis B, Environmental* 2009, **89**(3-4)**:**398-405.

190. Khan R, Kim SW, Kim TJ, Nam CM: **Comparative study of the photocatalytic performance of boron-iron Co-doped and boron-doped TiO2 nanoparticles.** *Materials Chemistry & Physics* 2008, **112**(1)**:**167-172.

191. Lu N, Zhao H, Li J, Quan X, Chen S: **Characterization of boron-doped TiO2 nanotube arrays prepared by electrochemical method and its visible light activity.** *Separation and Purification Technology* 2008, **62**(3)**:**668-673.

192. Lu N, Quan X, Li J, Chen S, Yu H, Chen G: **Fabrication of Boron-Doped TiO2 Nanotube Array Electrode and Investigation of Its Photoelectrochemical Capability.** *Journal of Physical Chemistry C* 2007, **111**(32)**:**11836-11842.

193. Zaleska A, Sobczak JW, Grabowska E, Hupka J: **Preparation and photocatalytic activity of boron-modified TiO2 under UV and visible light.** *Applied Catalysis B, Environmental* 2008, **78**(1-2)**:**92-100.

194. Jin C, Zheng RY, Guo Y, Xie JL, Zhu YX, Xie YC: **Hydrothermal synthesis and characterization of phosphorous-doped TiO2 with high photocatalytic activity for methylene blue degradation.** *Journal of Molecular Catalysis.A, Chemical* 2009, **313**(1-2)**:**44-48.

195. JIN C, QIU S, ZHU Y, XIE Y: **Phosphorous-Modified TiO2 with Excellent Thermal Stability and Its Application to the Degradation of Pollutants in Water.** *Chinese Journal of Catalysis* 2011, **32**(6-8)**:**1173-1179.

196. Lien SY, Wu BR, Mao HY, Wang JH, Hsieh IC, Yao PC, Wuu DS: **Simultaneous recrystallization, phosphorous diffusion and antireflection coating of silicon films using laser treatment.** *Thin Solid Films* 2006, **496**(2)**:**643-648.

197. Shen Y, Xiong T, Du H, Jin H, Shang J, Yang K: **Phosphorous, nitrogen, and molybdenum ternary co-doped TiO2: preparation and photocatalytic activities under visible light.** *J Sol-Gel Sci Technol* 2009, **50**(1)**:**98-102.

198. Wang X, Wang C, Jiang W, Guo W, Wang J: **Sonochemical synthesis and characterization of Cl-doped TiO2 and its application in the photodegradation of phthalate ester under visible light irradiation.** *Chemical Engineering Journal* 2012, **189-190:**288-294.

199. Xu H, Zheng Z, Zhang L, Zhang H, Deng F: **Hierarchical chlorine-doped rutile TiO2 spherical clusters of nanorods: Large-scale synthesis and high photocatalytic activity.** *Journal of Solid State Chemistry* 2008, **181**(9)**:**2516-2522.

200. Xu H, Zhang L: **Selective Nonaqueous Synthesis of C-Cl-Codoped TiO2 with Visible-Light Photocatalytic Activity.** *J Phys Chem C* 2010, **114**(26)**:**11534-11541.

201. Czoska AM, Livraghi S, Chiesa M, Agnoli S, Granozzi G, Finazzi E, Valentin CD, Pacchioni G, Giamello E: **The Nature of Defects in Fluorine-Doped TiO2.** *Journal of Physical Chemistry C* 2008, **112**(24)**:**8951-8956.

202. Li D, Haneda H, Labhsetwar NK, Hishita S, Ohashi N: **Visible-light-driven photocatalysis on fluorine-doped TiO2 powders by the creation of surface oxygen vacancies.** *Chemical Physics Letters* 2005, **401**(4-6)**:**579-584.

203. Yamaki T, Umebayashi T, Sumita T, Yamamoto S, Maekawa M, Kawasuso A, Itoh H: **Fluorine-doping in titanium dioxide by ion implantation technique.** *Nuclear Instruments and Methods in Physics Research Section B: Beam Interactions with Materials and Atoms* 2003, **206:**254-258.

204. Yu JC, Yu J, Ho W, Jiang Z, Zhang L: **Effects of F- Doping on the Photocatalytic Activity and Microstructures of Nanocrystalline TiO2 Powders.** *Chemistry of Materials* 2002, **14**(9)**:**3808-3816.

205. Nakamura R, Tanaka T, Nakato Y: **Mechanism for Visible Light Responses in Anodic Photocurrents at N-Doped TiO2 Film Electrodes.** *The Journal of Physical Chemistry B* 2004, **108**(30)**:**10617-10620.

206. Sakthivel S, Kisch H: **Daylight Photocatalysis by Carbon-Modified Titanium Dioxide.** *Angew Chem Int Ed* 2003, **42**(40)**:**4908-4911.

207. Xu C, Killmeyer R, Gray ML, Khan SUM: **Photocatalytic effect of carbon-modified n-TiO2 nanoparticles under visible light illumination.** *Applied Catalysis B: Environmental* 2006, **64**(3–4)**:**312-317.

208. Wong MS, Hsu SW, Rao KK, Kumar CP: **Influence of crystallinity and carbon content on visible light photocatalysis of carbon doped titania thin films.** *Journal of Molecular Catalysis.A, Chemical* 2008, **279**(1)**:**20-26.

209. Sakthivel S, Janczarek M, Kisch H: **Visible Light Activity and Photoelectrochemical Properties of Nitrogen-Doped TiO2.** *The Journal of Physical Chemistry B* 2004, **108**(50)**:**19384-19387.

210. Chen Q, Jiang D, Shi W, Wu D, Xu Y: **Visible-light-activated Ce–Si co-doped TiO2 photocatalyst.** *Appl Surf Sci* 2009, **255**(18)**:**7918-7924.

211. Ni M, Leung MKH, Leung DYC, Sumathy K: **A review and recent developments in photocatalytic water-splitting using for hydrogen production.** *Renewable and Sustainable Energy Reviews* 2007, **11**(3)**:**401-425.

212. Ho W, Yu JC: **Sonochemical synthesis and visible light photocatalytic behavior of CdSe and CdSe/TiO2 nanoparticles.** *Journal of Molecular Catalysis.A, Chemical* 2006, **247**(1-2)**:**268-274.

213. Wu L, Yu JC, Fu X: **Characterization and photocatalytic mechanism of nanosized CdS coupled TiO2 nanocrystals under visible light irradiation.** *Journal of Molecular Catalysis.A, Chemical* 2006, **244**(1-2)**:**25-32.

214. L S, H W, A H: **Photochemistry of semiconductor colloids. 22. Electron ejection from illuminated cadmium sulfide into attached titanium and zinc oxide particles.** *Journal of the American Chemical Society* 1987, **109**(22)**:**6632 -6635.

215. Bessekhouad Y, Robert D, Weber JV: **Bi2S3/TiO2 and CdS/TiO2 heterojunctions as an available configuration for photocatalytic degradation of organic pollutant.** *J Photochem Photobiol A* 2004, **163**(3)**:**569-580.

216. Baker DR, Kamat PV: **Photosensitization of TiO2 Nanostructures with CdS Quantum Dots: Particulate versus Tubular Support Architectures.** *Adv Funct Mater* 2009, **19**(5)**:**805-811.

217. Bessekhouad Y, Chaoui N, Trzpit M, Ghazzal N, Robert D, Weber JV: **UV-vis versus visible degradation of Acid Orange II in a coupled CdS/TiO2 semiconductors suspension.** *Journal of Photochemistry & Photobiology, A: Chemistry* 2006, **183**(1-2)**:**218-224.

218. Reutergårdh LB, Iangphasuk M: **Photocatalytic decolourization of reactive azo dye: a comparison between TiO2 and CdS photocatalysis.** *Chemosphere* 1997, **35**(3)**:**585-596.

219. Sun W, Yu Y, Pan H, Gao X, Chen Q, Peng L: **CdS Quantum Dots Sensitized TiO2 Nanotube-Array Photoelectrodes.** *J Am Chem Soc* 2008, **130**(4)**:**1124-1125.

220. Wu L, Yu JC, Fu X: **Characterization and photocatalytic mechanism of nanosized CdS coupled TiO2 nanocrystals under visible light irradiation.** *Journal of Molecular Catalysis.A, Chemical* 2006, **244**(1-2)**:**25-32.

221. Peter LM, Riley DJ, Tull EJ, Wijayantha KGU: **Photosensitization of nanocrystalline TiO2 by self-assembled layers of CdS quantum dots.** *Chemical Communications* 2002, **2002**(10)**:**1030-1031.

222. Yu JC, Wu L, Lin J, Li P, Li Q: **Microemulsion-mediated solvothermal synthesis of nanosized CdS-sensitized TiO2 crystalline photocatalyst.** *Chemical Communications* 2003, **2003**(13)**:**1552-1553.

223. Yang J, Li D, Wang X, Yang X, Lu L: **Rapid Synthesis of Nanocrystalline TiO2/SnO2 Binary Oxides and Their Photoinduced Decomposition of Methyl Orange.** *Journal of Solid State Chemistry* 2002, **165**(1)**:**193-198.

224. Vinodgopal K, Bedja I, Kamat PV: **Nanostructured Semiconductor Films for Photocatalysis. Photoelectrochemical Behavior of SnO2/TiO2 Composite Systems and Its Role in Photocatalytic Degradation of a Textile Azo Dye.** *Chemistry of Materials* 1996, **8**(8)**:**2180-2187.

225. Vinodgopal K, Kamat PV: **Enhanced Rates of Photocatalytic Degradation of an Azo Dye Using SnO2/TiO2 Coupled Semiconductor Thin Films.** *Environ Sci Technol* 1995, **29**(3)**:**841-845.

226. Anderson C, Bard AJ: **Improved Photocatalytic Activity and Characterization of Mixed TiO2/SiO2 and TiO2/Al2O3 Materials.** *The Journal of Physical Chemistry B* 1997, **101**(14)**:**2611-2616.

227. Chun H, Yizhong W, Hongxiao T: **Preparation and characterization of surface bond-conjugated TiO2/SiO2 and photocatalysis for azo dyes.** *Applied Catalysis B: Environmental* 2001, **30**(3-4)**:**277-285.

228. Machida M, Norimoto K, Watanabe T, Hashimoto K, Fujishima A: **The effect of SiO2 addition in super-hydrophilic property of TiO2 photocatalyst.** *J Mater Sci* 1999, **34**(11)**:**2569-2574.

229. Noh HN, Myong SY: **Antireflective coating using a WO3–TiO2 nanoparticle photocatalytic composition for high efficiency thin-film Si photovoltaic modules.** *Solar Energy Mater Solar Cells* 2014, **121**(0)**:**108-113.

230. Wang T, Tang J, Wu S, Fan X, He J: **Preparation of ordered mesoporous WO3–TiO2 films and their performance as functional Pt supports for synergistic photo-electrocatalytic methanol oxidation.** *J Power Sources* 2014, **248**(0)**:**510-516.

231. Ramos-Delgado NA, Gracia-Pinilla MA, Maya-Treviño L, Hinojosa-Reyes L, Guzman-Mar JL, Hernández-Ramírez A: **Solar photocatalytic activity of TiO2 modified with WO3 on the degradation of an organophosphorus pesticide.** *J Hazard Mater* 2013, **263, Part 1**(0)**:**36-44.

232. Lu S, Wang Q, Stevens WR, Lee CW, Gullett BK, Zhao Y: **Study on the decomposition of trace benzene over V2O5–WO3/TiO2-based catalysts in simulated flue gas.** *Applied Catalysis B: Environmental* 2014, **147**(0)**:**322-329.

233. Kovács G, Baia L, Vulpoi A, Radu T, Karácsonyi É, Dombi A, Hernádi K, Danciu V, Simon S, Pap Z: **TiO2/WO3/Au nanoarchitectures' photocatalytic activity, "from degradation intermediates to catalysts' structural peculiarities", Part I: Aeroxide P25 based composites.** *Applied Catalysis B: Environmental* 2014, **147**(0)**:**508-517.

234. Han D, Choi D, Park J: **Al2O3/TiO2 multilayer thin films grown by plasma enhanced atomic layer deposition for organic light-emitting diode passivation.** *Thin Solid Films* (0)**:**.

235. Zhao J, Wang Y, Lou X, Li K, Li Z, Huang W: **Effects of adding Al2O3 on the crystal structure of TiO2 and the performance of Pd-based catalysts supported on the composite for the total oxidation of ethanol.** *Inorg Chim Acta* 2013, **405**(0)**:**395-399.

236. Yiamsawas T, Mahian O, Dalkilic AS, Kaewnai S, Wongwises S: **Experimental studies on the viscosity of TiO2 and Al2O3 nanoparticles suspended in a mixture of ethylene glycol and water for high temperature applications.** *Appl Energy* 2013, **111**(0)**:**40-45.

237. Akkaya Arıer UO, Tepehan FZ: **Influence of Al2O3:TiO2 ratio on the structural and optical properties of TiO2–Al2O3 nano-composite films produced by sol gel method.** *Composites Part B: Engineering* 2014, **58**(0)**:**147-151.

238. Liu X, Hu Y, Chen R, Chen Z, Han H: **Coaxial Nanofibers of ZnO-TiO2 Heterojunction With High Photocatalytic Activity by Electrospinning Technique.** *Synthesis and Reactivity in Inorganic, Metal-Organic, and Nano-Metal Chemistry* 2014, **44**(3)**:**449-453.

239. Du P, Song L, Xiong J, Cao H: **Photocatalytic degradation of Rhodamine B using electrospun TiO2 and ZnO nanofibers: a comparative study.** *J Mater Sci* 2013, **48**(24)**:**8386-8392.

240. Jlassi M, Chorfi H, Saadoun M, Bessaïs B: **ZnO ratio-induced photocatalytic behavior of TiO2–ZnO nanocomposite.** *Superlattices and Microstructures* 2013, **62**(0)**:**192-199.

241. Arun K, Kumar D, Murugesh M: **Effect of TiO2 and ZnS fillers on the bearing strength of gfrp composites.** *J Reinf Plast Compos* 2012, **31**(16)**:**1088-1096.

242. Labiadh H, Chaabane TB, Balan L, Becheik N, Corbel S, Medjahdi G, Schneider R: **Preparation of Cu-doped ZnS QDs/TiO2 nanocomposites with high photocatalytic activity.** *Applied Catalysis B: Environmental* 2014, **144**(0)**:**29-35.

243. Arun KV, Sujay Kumar D, Murugesh MC: **Influence of bolt configuration and TiO2/ZnS fillers content on the strength of composites fasteners.** *Mater Des* 2014, **53**(0)**:**51-57.

244. Kanda S, Akita T, Fujishima M, Tada H: **Facile synthesis and catalytic activity of MoS2/TiO2 by a photodeposition-based technique and its oxidized derivative MoO3/TiO2 with a unique photochromism.** *J Colloid Interface Sci* 2011, **354**(2)**:**607-610.

245. Tacchini I, Terrado E, Ansón A, Martínez MT: **Preparation of a TiO2-MoS2 nanoparticle-based composite by solvothermal method with enhanced photoactivity for the degradation of organic molecules in water under UV light.** *IET Micro&Nano Letters* 2011, **6**(11)**:**932-936.

246. Liu Q, Pu Z, Asiri A, Qusti A, Al-Youbi A, Sun X: **One-step solvothermal synthesis of MoS2/TiO2 nanocomposites with enhanced photocatalytic H2 production.** *J Nanopart Res* 2013, **15**(11)**:**1-7.

247. Ho W, Yu JC, Lin J, Yu J, Li P: **Preparation and Photocatalytic Behavior of MoS2 and WS2 Nanocluster Sensitized TiO2.** *Langmuir* 2004, **20**(14)**:**5865-5869.

248. Weijia Zhou, Zongyou Yin, Yaping Du, Xiao Huang, Zhiyuan Zeng, Zhanxi Fan, Hong Liu, Jiyang Wang, Hua Zhang: **Synthesis of Few-Layer MoS2 Nanosheet-Coated TiO2 Nanobelt Heterostructures for Enhanced Photocatalytic Activities.** *Small* 2013, **9**(1)**:**140-147.

249. N. Alonso Vante , W. Jaegermann , H. Tributsch , W. Hoenle , K. Yvon: **Electrocatalysis of oxygen reduction by chalcogenides containing mixed transition metal clusters.** 1987, **109**(11)**:**3251-3257.

250. Yamaguchi Y, Takeuchi T, Sakaebe H, Kageyama H, Senoh H, Sakai T, Tatsumi K: **Ab Initio Simulations of Li/Pyrite-MS2 (M = Fe, Ni) Battery Cells.** *J Electrochem Soc* 2010, **157**(6)**:**A630-A635.

251. W. F. Hillebrand: **THE VANADIUM SULPHIDE, PATRONITE, AND ITS MINERAL ASSOCIATES FROM MINASRAGRA, PERU..** *Journal of the American Chemical Society* 1907, **29:**1019-1029.

252. Allmann R, Baumann I, Kutoglu A, Rösch H, Hellner E: **Die Kristallstruktur des Patronits V(S2)2.** *Naturwissenschaften* 1964, **51**(11)**:**263-264.

253. Rout CS, Kim B, Xu X, Yang J, Jeong HY, Odkhuu D, Park N, Cho J, Shin HS: **Synthesis and Characterization of Patronite Form of Vanadium Sulfide on Graphitic Layer.** *J Am Chem Soc* 2013, **135**(23)**:**8720-8725.

254. Masao Yokoyama, Masahiro Yoshimura, Masataka Wakihara, Shigeyuki Somiya, Masao Taniguchi: **Synthesis of vanadium sulfides under high pressure.** *Journal of Solid State Chemistry* 1985, **60**(2)**:**182-187.

255. Taniguchi M, Wakihara M, Shirai Y: **Growth of Single Crystals of Vanadium Sulfides and their electrical conductivity.** *Z Anorg Allg Chem* 1980, **461**(1)**:**234-240.

256. Murugesan T, Ramesh S, Gopalakrishnan J, Rao CNR: **Ternary vanadium sulfides.** *Journal of Solid State Chemistry* 1982, **44**(1)**:**119-125.

257. Lui G, Liao J, Duan A, Zhang Z, Fowler M, Yu A: **Graphene-wrapped hierarchical TiO2 nanoflower composites with enhanced photocatalytic performance.** *Journal of Materials Chemistry a* 2013, **1**(39)**:**12255-12262.

258. Bakardjieva S, Subrt J, Stengl V, Dianez MJ, Sayagues MJ: **Photoactivity of anatase-rutile TiO2 nanocrystalline mixtures obtained by heat treatment of homogeneously precipitated anatase.** *Applied Catalysis B: Environmental* 2005, **58**(3-4)**:**193-202.

259. Zhang H, Lv X, Li Y, Wang Y, Li J: **P25-Graphene Composite as a High Performance Photocatalyst.** *ACS Nano* 2010, **4**(1)**:**380-386.

260. Tauc J, Grigorovici R, Vancu A: **Optical Properties and Electronic Structure of Amorphous Germanium.** *phys stat sol (b)* 1966, **15**(2)**:**627-637.

261. Lin H, Huang CP, Li W, Ni C, Shah SI, Tseng YH: **Size dependency of nanocrystalline TiO2 on its optical property and photocatalytic reactivity exemplified by 2-chlorophenol.** *Applied Catalysis B, Environmental* 2006, **68**(1-2)**:**1-11.